Human Molecular Genetics, 2008, Vol. 17, No. 14 **2084–2100**
doi:10.1093/hmg/ddn107
Advance Access published on April 1, 2008

Therapeutic benefit derived from RNAi-mediated ablation of IMPDH1 transcripts in a murine model of autosomal dominant retinitis pigmentosa (RP10)

Lawrence C.S. Tam[1,*], Anna-Sophia Kiang[1], Avril Kennan[1], Paul F. Kenna[1], Naomi Chadderton[1], Marius Ader[1], Arpad Palfi[1], Aileen Aherne[1], Carmen Ayuso[2], Matthew Campbell[1], Alison Reynolds[1], Alex McKee[1], Marian M. Humphries[1], G. Jane Farrar[1] and Pete Humphries[1]

[1]The Ocular Genetics Unit, Department of Genetics, Trinity College Dublin, Dublin 2, Ireland and [2]Genetics Department, Fundacion Jimenez Diaz-CIBERER, Madrid, Spain

Received February 15, 2008; Revised and Accepted March 29, 2008

Mutations within the inosine 5′-monophosphate dehydrogenase 1 (IMPDH1) gene cause the RP10 form of autosomal dominant retinitis pigmentosa (adRP), an early-onset retinopathy resulting in extensive visual handicap owing to progressive death of photoreceptors. Apart from the prevalence of RP10, estimated to account for 5–10% of cases of adRP in United States and Europe, two observations render this form of RP an attractive target for gene therapy. First, we show that while recombinant adeno-associated viral (AAV)-mediated expression of mutant human IMPDH1 protein in the mouse retina results in an aggressive retinopathy modelling the human counterpart, expression of a normal human IMPDH1 gene under similar conditions has no observable pathological effect on retinal function, indicating that over-expression of a therapeutic replacement gene may be relatively well tolerated. Secondly, complete absence of IMPDH1 protein in mice with a targeted disruption of the gene results in relatively mild retinal dysfunction, suggesting that significant therapeutic benefit may be derived even from the suppression-only component of an RNAi-based gene therapy. We show that AAV-mediated co-expression in the murine retina of a mutant human IMPDH1 gene together with short hairpin RNAs (shRNA) validated *in vitro* and *in vivo*, targeting both human and mouse IMPDH1, substantially suppresses the negative pathological effects of mutant IMPDH1, at a point where, in the absence of shRNA, expression of mutant protein in the RP10 model essentially ablates all photoreceptors in transfected areas of the retina. These data strongly suggest that an RNAi-mediated approach to therapy for RP10 holds considerable promise for human subjects.

INTRODUCTION

Globally, an estimated 161 million people are visually handicapped, among which approximately 37 million have the status of legal blindness, with visual acuity of less than 6/20, and corresponding visual field loss of $<20^{\circ}$ (World Health Organization; http://www.who.int/en). The most prevalent causes of blindness are cataract, glaucoma and age-related macular dystrophy (AMD), the latter, involving degeneration of the central retina (macula) and primarily a disease of the elderly, representing by far the most common cause of registered blindness in the developed world. The hereditary retinopathy, retinitis pigmentosa (RP) is, however, the most common cause of registered visual handicap among those of working age in developed countries. Hence the social and economic impact of this condition is particularly high. RP is a highly variable disorder where patients may develop symptomatic visual loss in early childhood, while others may remain asymptomatic until mid-adulthood (1). In most cases, death of rod photoreceptor neurons results in nyctalopia (night blindness), and subsequently, progressive cone cell death causes constriction and often complete loss of visual fields. Most cases of RP segregate in autosomal dominant, recessive or X-linked recessive modes and approximately 40 genes have been implicated in disease pathology to date (http:www.sph.uth.tmc.edu/RetNet). The extensive genetic

*To whom correspondence should be addressed. Tel: +353 18962486; Fax: +353 18963848; Email: lawrenct@tcd.ie

heterogeneity associated with autosomal dominant RP (adRP) is an undisputed hindrance to the development of genetically-based therapeutics for primary genetic lesions, where therapies involving the targeting of individual genes will require development. However, some forms of disease are likely to represent more attractive initial therapeutic targets than others, owing to features associated with their molecular pathologies. Arguably, one such disease is the RP10 form of adRP. The gene was initially localized in 1993 (2), but it was not until 2002, as a result of global transcriptional analysis of normal and degenerating ($Rho^{-/-}$ and $Crx^{-/-}$) retinas, that mutations within the inosine 5′-monophosphate dehydrogenase 1 (IMPDH1) gene were associated with the disease (3,4). IMPDH1 is a rate-limiting enzyme in the *de novo* biosynthesis pathway for guanine nucleotides. Enzymes of the nucleotide biosynthesis pathways are important in supporting many cellular functions and play crucial regulatory roles in the phototransduction cascade. In humans, IMPDH activity is governed by two separate but very closely related isoforms, termed type I and II, which share similar enzymatic activities (5–8). The two types of IMPDH mRNA are expressed over a wide range of tissues and are differentially regulated in proliferating cells (9–11). Thus, IMPDH1 is one of a small group of proteins which are expressed in a wide number of tissues and yet, when mutated, result in disease pathology only in the retina. Previous studies on the biochemical properties of mutant IMPDH1 proteins bearing the common missense mutations, Arg224Pro and Asp226Asn, together with computational modelling simulations, have indicated that mutant IMPDH1 has a tendency to aggregate, and thus photoreceptor cell death may be caused as a result of this phenomenon (12). Additional studies have also shown that pathogenic mutations negatively affect the specificity and affinity of IMPDH1 enzyme to bind single nucleic acids (13,14), although the functional consequences, if any, in respect to disease pathology, remain to be elucidated. In a recent study, it has been shown that both human and mouse photoreceptor cells express multiple IMPDH1 transcripts that give rise to different protein isoforms (15). These isoforms generated through alternative splicing may disrupt other nucleic acid metabolisms in photoreceptor cells. However, the fact that IMPDH1 knockout mice fail to display a retinal pathology suggests that mutations encountered within the gene in adRP exert a dominant negative effect on phenotype.

RP10 is a particularly severe form of adRP, with significant loss of visual acuity and visual fields usually occurring within the second decade of life. The disease is estimated to represent 5–10% of cases of adRP in the American and European populations (16), and on prevalence grounds alone, the condition is well worth targeting. However, two features of the disease appear to render it particularly suitable for explorations of therapeutic intervention. First, while we show here that a severe retinopathy mimicking the human counterpart can be induced in the mouse retina following sub-retinal inoculation of a recombinant adeno-associated virus (rAAV) expressing a rod-opsin promoter-driven mutant form of the human gene, expression of a wild-type (WT) gene under similar conditions appears to have little negative pathological effect. Moreover, we have shown that mice with a targeted disruption of the IMPDH1 gene ($IMPDH1^{-/-}$) develop only an exceedingly mild retinopathy, with electroretinographic (ERG) waveforms still detectable and the bulk of the outer nuclear layer (ONL) of the retina remaining intact, at 2 years of age (12). These data strongly suggest that therapeutic benefit may well be derived by simultaneous co-suppression of both normal and mutant IMPDH1 alleles and that, should a replacement gene be required, over- or under-expression of it may be tolerated without significant detrimental effect on retinal structure or function. In this context, we describe the effective and sequence-specific suppression of human and mouse IMPDH1 at both the mRNA and protein levels by small interfering/short hairpin RNAs (si/shRNAs) in mammalian cell culture, *ex vivo* in murine retinal explants and in mouse *in vivo*. In particular, we show that the retinopathy induced in WT mice by expression of a mutant human IMPDH1 gene can be significantly ameliorated by co-expression of an shRNA molecule targeting mouse and human IMPDH1 transcripts, at a point at which untreated animals in the RP10 model display essentially complete photoreceptor ablation in transfected areas of retina. These studies provide a structured basis for the further development of a genetic means of therapy for this severe form of visual handicap.

RESULTS

Design of siRNAs targeting human and mouse IMPDH1 transcripts

In order to select distinct siRNA target sites on human and mouse IMPDH1 transcripts, the human IMPDH1 mRNA sequence was submitted to siRNA target selection softwares provided by Dharmacon (www.dharmacon.com), and recommended target sites were then aligned against the mouse IMPDH1 mRNA sequence to select homologous regions between both human and mouse IMPDH1 transcripts. Two optimal siRNAs, termed si1224 and si2048 (Fig. 1A), specific for only human and both human and mouse IMPDH1 transcripts, respectively, were then selected on the basis of compliance with additional criteria (17) and of having minimal regions of sequence complementarity to IMPDH2.

siRNA-mediated suppression of IMPDH1 transcripts in mammalian cell culture

To evaluate the suppression efficiency of siRNAs, HeLa cells were separately transfected with 20 pmol of si1224 and si2048, and the level of endogenous human IMPDH1 transcripts was quantified and compared with that of luciferase GL3-targeting siRNA (siLuc) transfected cells by real-time RT–PCR. siRNAs targeting two sequence variants of firefly (*Photinus pyralis*, GL2 and GL3) luciferase (18) have previously been used as non-targeting controls in other RNAi studies where they showed minimum silencing effects on unrelated genes (19,20). Twenty-four hours post-transfection, si1224 and si2048 reduced endogenous IMPDH1 mRNA levels to 31 ± 7.24 and $25 \pm 2.98\%$, respectively, compared with siLuc controls ($P \leq 0.0001$; Fig. 1B). Co-transfection of si1224 and si2048 suppressed endogenous IMPDH1 mRNA to $20 \pm 2.25\%$ ($P \leq 0.0001$), compared with the control (Fig. 1B), but this did not differ significantly from transfection by si2048 alone ($P = 0.095$).

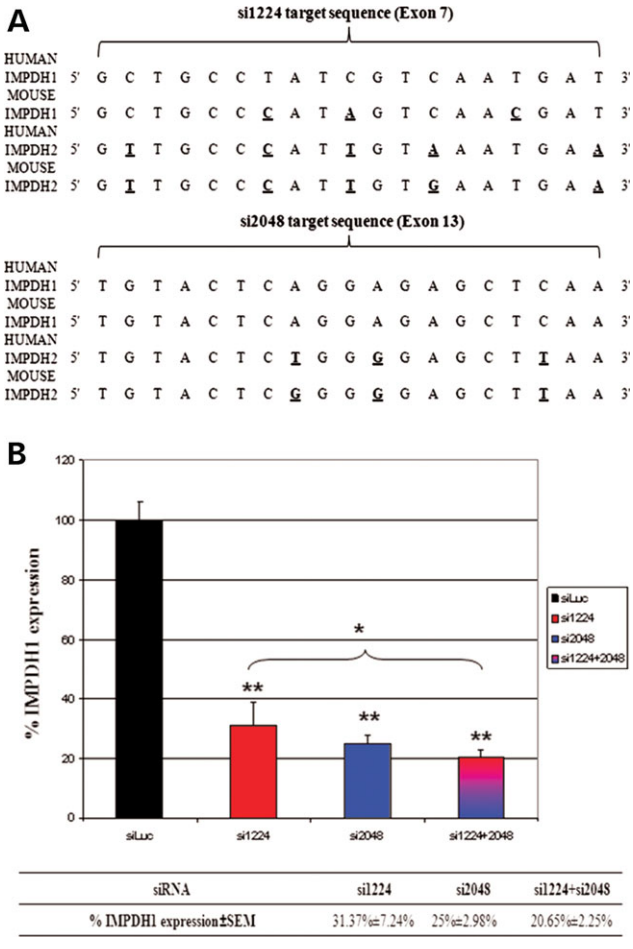

Figure 1. Design and assessment of IMPDH1-specific siRNAs in mammalian cell culture. (**A**) Alignments of siRNA target sites on human IMPDH1 (GenBank accession no. NM_000883) against mouse IMPDH1 (GenBank accession no. BC053416), human IMPDH2 (GenBank accession no. NM_000884) and mouse IMPDH2 (GenBank accession no. BC052671). Sequence alignment was carried out using Clustal W multiple sequence alignment (http://www.ebi.ac.uk/clustalw). Mismatches between siRNA and target sequences are in bold and underlined. (**B**) siRNA-mediated suppression of endogenous IMPDH1 mRNA expression in HeLa cells. HeLa cells were separately transfected with 20 pmol of siRNAs (si1224 and si2048), or in combinations (total concentration = 20 pmol). Percentage IMPDH1 expression was quantified by real-time RT–PCR and normalized to β-actin mRNA. Y-error bars indicate standard error of the mean (SEM). $^{*}P < 0.05$ and $^{**}P \leq 0.0001$. siLuc, siLuciferaseGL3.

Down-regulation of IMPDH1 by shRNA in mammalian cell culture

Although the two synthetic IMPDH1-specific siRNAs have been shown to be effective in suppressing IMPDH1 at the mRNA level in mammalian cells, the transient silencing effect and high-cost of production associated with synthetic siRNAs greatly reduces their applicability in long-term *in vivo* studies. To overcome this limitation, oligonucleotides based on the sequences of the two synthetic IMPDH1-specific siRNAs (si1224 and si2048) were generated (Table 1), annealed and cloned into the pBluescriptH1 RNAi-vector system to enable the generation of shRNAs *in vivo* (Fig. 2A). As can be seen in Figure 2B, suppression efficiency was retained in the pBluescriptH1 vector system where both sh1224 and sh2048 significantly reduced endogenous IMPDH1 transcripts in HeLa cells to 24 ± 3.13 and $16 \pm 2.19\%$, respectively, compared with the shLuc control ($P = 0.0012$ and $P = 0.0014$, respectively). Furthermore, the capacity of both sh1224 and sh2048 to silence WT and mutant IMPDH1 protein expression was also retained, quantification of band intensities showing that sh1224 and sh2048 significantly reduced exogenous WT IMPDH1 protein expression to 23 and 17%, respectively (Fig. 2C), and reduced IMPDH1 mutant Arg224Pro to 14 and 12% respectively (Fig. 2D; $P = 0.0112$ and $P = 0.0217$, respectively) and IMPDH1 mutant Asp226Asn to 29 and 22% respectively (Fig. 2E; $P \leq 0.05$ and $P \leq 0.0001$, respectively). Taken together, these data demonstrate that H1-directed synthesis of shRNAs can mediate gene silencing of WT and mutant IMPDH1 in cell culture with efficiency comparable to that of the synthetic counterparts.

shRNA-mediated suppression of IMPDH1 *ex vivo* in mouse retinal explants

In order to conveniently test the efficacy of shRNA-mediated IMPDH1 suppression in retinal tissue without the need to first optimize delivery to mouse eyes, constructs expressing

Table 1. Sequences of IMPDH1-specific shRNAs and synthetic siRNAs, and non-targeting control si/shRNAs

si/shRNA name		Target positions on human IMPDHI (NM_000883)	Sequences 5′→3′
si1224	Sense	1224–1242	gcugccuaucgucaaugau
	Antisense		aucauugacgauaggcagc
si2048	Sense	2048–2066	uguacucaggagagcucaa
	Antisense		uugagcucuccugaguaca
sh1224	Sense	1224–1242	gatccccgctgcctatcgtcaatgatttcaagagaatcattgacgataggcagctttttta
	Antisense		agcttaaaaagctgcctatcgtcaatgattctcttgaaatcattgacgataggcagcggg
sh2048	Sense	2048–2066	gatcccctgtactcaggagagctcaatccaagagattgagctctcctgagtacatttttta
	Antisense		agcttaaaaatgtactcaggagagctcaatctcttgaattgagctctcctgagtacaggg
Non-targeting si/shRNA siLuciferase GL3 (siLuc)	Sense		cuuacgcugaguacgucga
	Antisense		ucgaaguacucagcguaag
shLuciferase GL2 (shLuc)	Sense		gatccccgcgtacggggaaacttcgattcaagagatcgaagtattccgcgtacgtttttggaa
	Antisense		agcttttccaaaaacgtacgcggaatacttcgatctcttgaatcgaagttttccccgtacgcggg

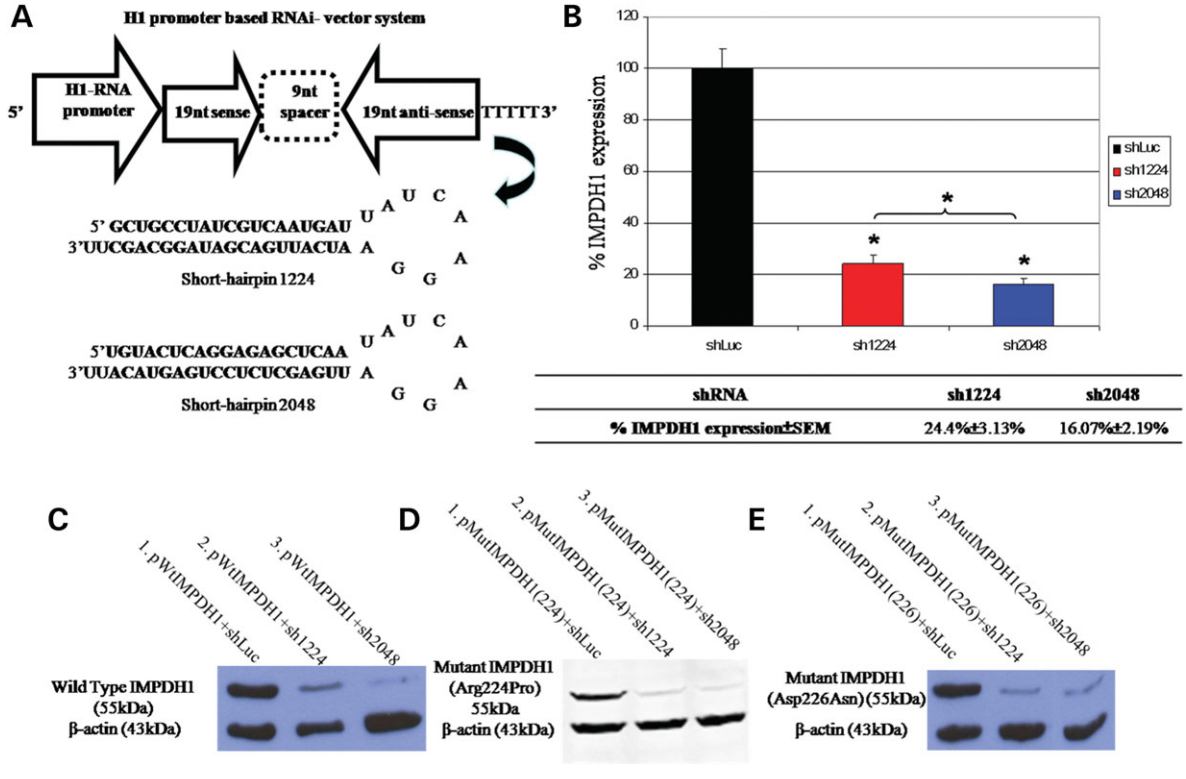

Figure 2. Short-hairpin RNAi-mediated suppression of IMPDH1 in mammalian cell culture. (**A**) Sub-cloning of shRNA oligonucleotides into pBluescriptH1 vector to construct the human H1 promoter driven vector for short hairpin RNA (66). (**B**) Suppression of endogenous IMPDH1 mRNA in HeLa cells by polymerase III H1-promoter driven shRNAs. HeLa cells were separately transfected with 1 μg/μl of psh1224 and psh2048 and the level of IMPDH1 mRNA expression was quantified by real-time RT–PCR 24 h post-transfection. Control cells were transfected with LuciferaseGL2-specific shRNAs, and IMPDH1 expression from these was standardized to represent 100% IMPDH1 (black bar). The average of 3 independent experiments is shown; Y-error bars indicate standard error of the mean (SEM). $^{*}P < 0.05$. Western blot analysis illustrating shRNA-mediated suppression of (**C**) wild-type IMPDH1 protein, (**D**) mutant IMPDH1 protein harbouring the Arg224Pro mutation and (**E**) mutant IMPDH1 protein harbouring the Asp226Asn mutation in HeLa cells.

shRNA tagged with enhanced green fluorescent protein (EGFP) (psh2048.EGFP and pshLuc.EGFP, Fig. 3A) were electroporated into mouse retinal explants. Previous studies carried out in our laboratory have successfully used an identical dual-expression RNAi vector system to express shRNAs targeting rhodopsin and *rds*/peripherin *ex vivo* in retinal explants (21–23).

One technical factor limiting the use of RNAi for studies of gene suppression in tissues is that many cell types are only transfected with low efficiency, resulting, unavoidably, in a

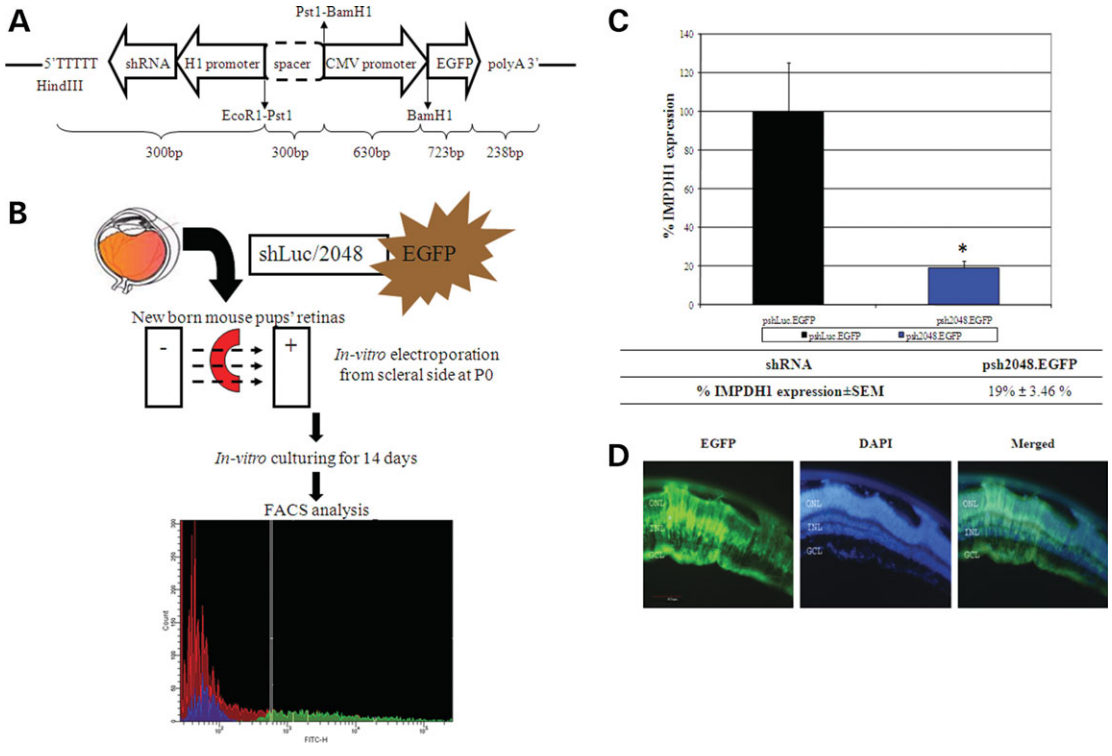

Figure 3. Down-regulation of IMPDH1 transcripts *ex vivo* in mouse retinal explants. (**A**) A schematic illustration of the dual-expression shRNA plasmid. Restriction fragments containing the H1 promoter, shRNA sequences and termination signal were excised from pshLuc and psh2048, respectively, and sub-cloned into pEGFP-1 (Clontech) containing the EGFP cDNA driven by the CMV promoter. (**B**) A schematic diagram illustrating the steps involved in the electroporation, maintenance, dissociation and fluorescence activated cell sorting (FACS) of cultured retinal explants. The histogram illustrates green fluorescence intensity (FITC, x-axis) versus cell number. Red bars represent cell population with fluorescence levels below an arbitrary level, whereas green bars denote those above an arbitrary fluorescence threshold. (**C**) Suppression of IMPDH1 transcripts in mouse retinal explants. Electroporated retinas were cultured for 14 days *in vitro*, pooled together before trypsin dissociation into single cell suspensions and dissociated retinal cells were FACS sorted. RNA was extracted from EGFP-positive retinal cells and percentage IMPDH1 mRNA expression was quantified by real-time RT–PCR analysis, and normalized to the housekeeping gene, β-actin. Y-error bars indicate standard error of the mean (SEM). $^{*}P < 0.05$ ($n = 12$). (**D**) *In vitro* electroporated mouse retinal explants at Day 14. WT C57B6/CBA mouse retinas at P0 were *in vitro* electroporated with psh2048.EGFP from the scleral side and cultured for 14 days. Scale bar: 40 μm. ONL, outer nuclear layer; INL, inner nuclear layer; GCL, ganglion cell layer.

large fraction of untransfected cells which contaminates the transfected population, thus diluting the observed RNAi effect and obscuring the experimental outcome. However, it is possible to obtain a pure transfectant population based on EGFP fluorescence using fluorescence-activated cell sorting (FACS) in which a heterogeneous mixture of cells are separated based upon the specific light scattering and fluorescent characteristics of each cell. Initially 12 retinas from new-born WT C57B6/CBA mouse pups were dissected and 6 retinas were separately electroporated in a pool within a micro-chamber containing 100 μl of pshLuc.EGFP or psh2048.EGFP at a concentration of 1 μg/μl, respectively. Retinal explants were then cultured *in vitro* for 14 days, and six retinas electroporated with each plasmid were pooled prior to trypsin dissociation. Trypsin-dissociated single retinal cells expressing EGFP, representing transfected cells were identified and underwent FACS analysis, i.e. electroporated retinal cells were sorted by size fractionation and EGFP fluorescence levels, in two independent experiments. The histogram of FITC versus cell number in Figure 3B shows that EGFP-fluorescent cells exhibited a >2 log-scale difference in their fluorescence level when compared with non-transfected cells, and accounted for ∼8–33% of the total cell population in two independent experiments. RNA was then extracted from the EGFP-positive retinal cells and the level of endogenous IMPDH1 mRNA in these cells positively transfected with psh2048.EGFP was shown to be significantly suppressed to 19 ± 3.46%, compared with levels found in cells transfected with the control, pshLuc.EGFP ($P = 0.0318$; Fig. 3C). In addition, the vibratome section illustrated in Figure 3D shows that 14-day-old electroporated retinal cultures differentiate and morphologically resemble a normal retina *in vivo*, displaying a defined ONL, inner nuclear layer and ganglion cell layer. Moreover, the CMV-driven EGFP reporter gene was expressed ubiquitously throughout the retina. In summary, these results validate the suppression of IMPDH1 in retinal tissue by RNAi.

Construction of rAAV-2/5 vectors expressing IMPDH1-specific shRNA and evaluation of *in vivo* transduction patterns

In order to generate an rAAV-based vector for shRNA delivery in this study, infectious recombinant human AAV-2 virions were generated using the AAV helper virus-free system (24). The expression element was inserted between

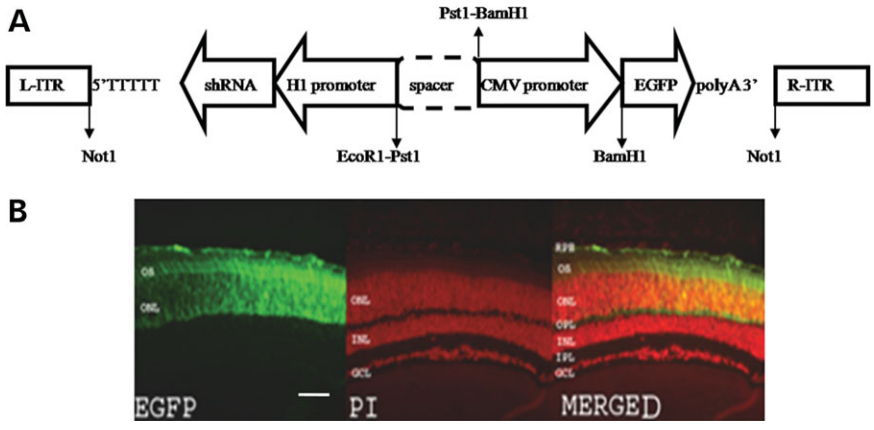

Figure 4. Design of recombinant adeno-associated viral vectors expressing IMPDH1-specific shRNA. (**A**) A schematic representation of pAAVshRNA.EGFP vector expressing either shLuc (non-targeting control) or sh2048 under the control of the human H1-promoter and an EGFP cDNA under the control of the CMV promoter. (**B**) Cryostat sections of 4-week-old WT C57B6/CBA mice (12 μm) sub-retinally injected with pAAVsh2048.EGFP. Scale bar: 40 μm. RPE, retinal pigment epithelium; OS, outer segment; ONL, outer nuclear layer; OPL, outer plexiform layer; INL, inner nuclear layer; IPL, inner plexiform layer; GCL, ganglion cell layer; PI, propidium iodide; merged, PI overlaid with EGFP.

the *cis*-acting AAV inverted terminal repeats, and AAV elements required for replication and packaging are provided *in-trans* on the plasmid pRep2/Cap5 (25), while a second plasmid, pHelper, provides the adenovirus gene products required for the production of infective AAV particles, such as E2A, E4 and VA RNA genes. The remaining adenoviral gene products are provided by the HEK-293 cells that stably express the adenovirus E1 gene. An rAAV-2/5 construct, designed to express both H1-promoter driven sh2048 and CMV promoter-driven EGFP (pAAVsh2048.EGFP), in order to suppress IMPDH1 and to allow for the direct identification of cells expressing shRNA in retina *in vivo* (Fig. 4A), was then packaged using the system described above. As an initial step to evaluate the transduction efficiency of rAAV-2/5 shRNA constructs, 3 μl (the maximum volume possible for sub-retinal injection) of pAAVsh2048.EGFP (2.19×10^{13} vp/ml) was sub-retinally injected into the right eye of a 4-week-old WT C57B6/CBA mouse, whereas the contralateral eye was injected with 3 μl of pAAVshLuc.EGFP (1×10^{13} vp/ml). Four weeks post-injection, the animal was sacrificed and isolated retinas were embedded in optimum cutting temperature solution (OCT) for cryostat sectioning. Upon examination under a fluorescent microscope, cryostat retinal sections injected with pAAVsh2048.EGFP showed strong EGFP signals in the retinal pigment epithelium (RPE), outer segments (OS) and ONL, whereas the inner nuclear layer and the ganglion cell layer were not transduced (Fig. 4B). In particular, rAAV-mediated expression of viral vectors did not disrupt the retinal structure. Furthermore, these results illustrated the specificity and efficiency of rAAV-2/5 vectors in transducing the RPE and photoreceptor cells, consistent with previous observations (26).

AAV-delivered RNAi-mediated suppression of IMPDH1 transcripts and protein *in vivo*

In order to assess long-term suppression of IMPDH1 *in vivo*, 1–3 μl of pAAVsh2048.EGFP (6.85×10^{12} vp/ml) was sub-retinally injected into the right eyes of adult WT C57B6/CBA mice, and contralateral eyes were injected with the same quantity of pAAVshLuc.EGFP in three independent experiments ($n = 20$). Four weeks post-injection, RNA was isolated from FACS-sorted EGFP-positive cells from the dissociated retinas, and real-time RT–PCR analysis undertaken. The results showed that, on average, AAV-sh2048 significantly reduced endogenous murine IMPDH1 expression to $22 \pm 3\%$, compared to the AAV-shLuc control ($P = 0.0271$; Fig. 5A).

Endogenous mouse IMPDH1 protein was first detected by western blot analysis using anti-N-IMPDH1 antibody, on native WT C57B6/CBA mouse retinal protein, and a single correctly sized band of 55 kDa was clearly visible as shown in Figure 5B. To evaluate the effect of AAV-expressed shRNA on the expression of IMPDH1 protein *in vivo*, adult WT C57B6/CBA mice were sub-retinally injected with 3 μl of pAAVsh2048.EGFP (6.85×10^{12} vp/ml) into the right eyes and with an equal amount of pAAVshLuc.EGFP into the contralateral eyes in three independent experiments ($n = 10$). In an attempt to maximize the area of rAAV transduction in the retina, a second sub-retinal injection was administered to a different area of the retina 1 week after the initial injection using the same concentrations of rAAV vectors (The 1 week gap was sufficient to allow the bleb formed by the first sub-retinal inoculation to settle before the second administration, thus minimizing damage to the retina). Four weeks after the second inoculation, total retinal protein was extracted and pooled for western blot analyses. Densitometric analysis of western blots from three independent experiments showed that AAV-sh2048 suppressed endogenous murine IMPDH1 protein to $22 \pm 6\%$ of that treated with the AAV-shLuc control (Fig. 5C).

Immunolocalization of IMPDH1 and immunohistochemical analysis of IMPDH1 suppression in mouse retina

Frozen fixed retinal sections from 1-month-old WT C57B6/CBA mice were immunofluorescently stained using

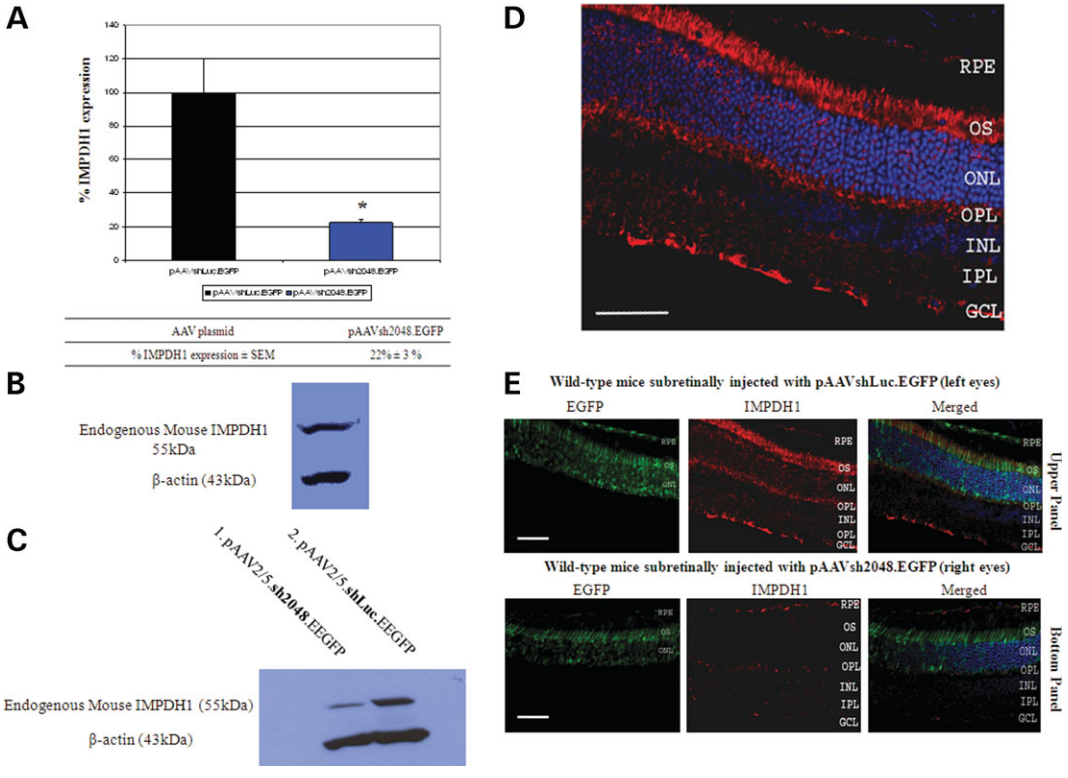

Figure 5. shRNA-mediated suppression of IMPDH1 *in vivo*. (**A**) rAAV-mediated suppression of endogenous IMPDH1 following FACS analysis in six 2-week-old WT C57B6/CBA mice sub-retinally injected with pAAVshLuc.EGFP (left eyes) and pAAVsh2048.EGFP (right eyes). Y-error bars denote standard error of the mean. $^{*}P < 0.05$. (**B**) Detection of endogenous mouse IMPDH1 in WT C57B6/CBA mouse retinas. (**C**) Western blot analysis of IMPDH1 protein expression in WT C57B6/CBA mouse retinas sub-retinally injected with rAAV vectors expressing sh2048 (lane 1) and shLuc (lane 2). (**D**) Immunolocalization of IMPDH1 in WT C57B6/CBA mouse retinas. Scale bar: 40 μm. (**E**) Immunohistochemical analysis of AAV-shRNA-mediated suppression of IMPDH1 in WT C57B6/CBA mouse retinas. Scale bar: 40 μm.

anti-C-IMPDH1 antibody, and immune complexes were detected with Cy3-labelled anti-rabbit IgG antibody. Anti-C-IMPDH1 staining shows that IMPDH1 localizes predominantly to the OS adjoining the ONL, while weaker staining in the RPE and synaptic terminals of the photoreceptor cells indicates that IMPDH1 is also present in these regions (Fig. 5D). This pattern of protein localization is consistent with the *in situ* mRNA expression pattern reported previously by Aherne *et al*. (12), and also with the immunofluorescence staining reported by Bowne *et al*. (15).

To qualitatively illustrate the levels of IMPDH1 protein reduction in shRNA-treated eyes, 3 μl of pAAVsh2048.EGFP (2.19×10^{13} vp/ml) was sub-retinally injected into 1-month-old WT C57B6/CBA mice, whereas contralateral eyes were injected with 3 μl of pAAVshLuc.EGFP (1×10^{13} vp/ml) ($n = 2$). Four weeks post-injection, sections from frozen retinas were probed with anti-C-IMPDH1 antibody and immune complexes were detected using Cy3-labelled anti-rabbit IgG antibody. Representative fluorescent images in Figure 5E showed near-complete suppression of IMPDH1 expression in the OS and ONL of retinas injected with pAAV-sh2048.EGFP (Fig. 5E, lower panels) compared with eyes injected with AAVshluc-targeting control (Fig. 5E, upper panels), which showed normal IMPDH1 expression patterns similar to those observed previously in Figure 5D. Collectively, these results demonstrate that AAV-sh2048 can elicit specific and potent silencing of IMPDH1 expression in the OS and ONL of injected mice.

Induction of retinopathy by AAV-mediated expression of mutant IMPDH1

We constructed rAAVs carrying either WT or mutant human IMPDH1 cDNAs driven by the human rhodopsin promoter and tagged with EGFP in order to study the effects of mutant IMPDH1 bearing the mutation Arg224Pro in murine retina in an attempt to model RP10 disease pathology. Three mircolitres of AAV-Mut224IMPDH1 (1.4×10^{12} vp/ml) were delivered sub-retinally to the right eyes of IMPDH1$^{+/-}$ mice ($n = 14$) at 8 weeks of age. The left eyes of the same animal received a similar quantity of AAV-WtIMPDH1 (3 μl of 1.77×10^{12} vp/ml). Four weeks later ERGs were performed on the animals which were subsequently sacrificed 2 days later and the eyes were resin-embedded for thin sectioning. Figure 6A illustrates the results from a representative ERG of this group of animals. Note the complete flattening of the maximal, dark-adapted combined rod and cone ERG response of the right eye which received AAV-Mut224IMPDH1 compared with the normal response of the AAV-WtIMPDH1-injected left eye. In addition, the histology clearly shows that in the right eye over an extensive region centering on the site of injection, the photoreceptor layer is

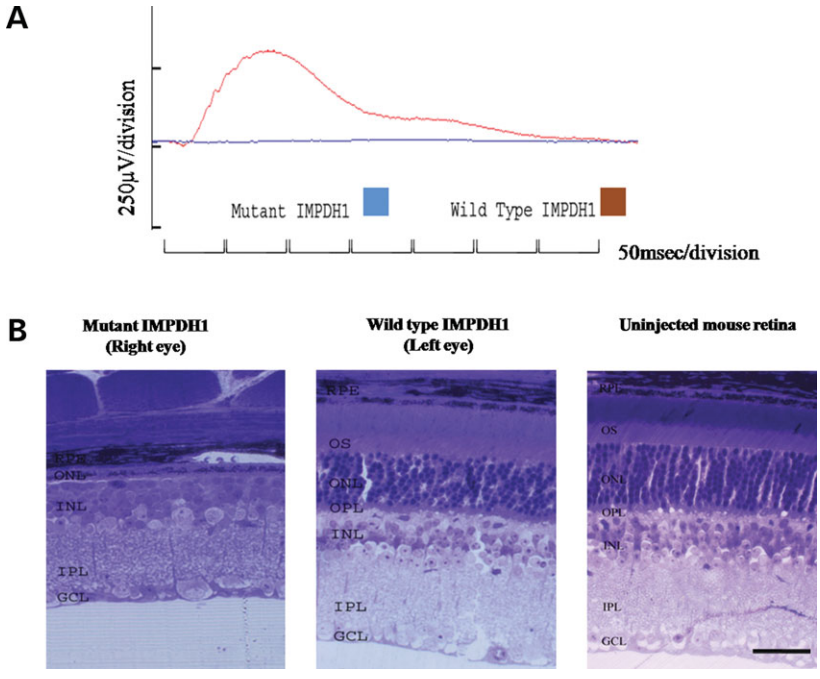

Figure 6. Induction of retinopathy in IMPDH1$^{+/-}$ mice by expression of mutant IMPDH1. (**A**) ERG analysis in IMPDH1$^{+/-}$ mice sub-retinally injected with rAAV-WT or mutant IMPDH1. Maximal, dark adapted, combined rod and cone response from IMPDH1$^{+/-}$ mice injected with either AAV-WT IMPDH1 (left eye) or AAV-mutant IMPDH1 (right eye) after 4 weeks of injection. (**B**) Light micrographs of resin embedded retinal sections (1μm) from a representative IMPDH1$^{+/-}$ mouse. Right eye was sub-retinally injected with AAV-mutant IMPDH1 harbouring the Arg224Pro mutation, and contralateral eye injected with AAV-WT IMPDH1. The outer nuclear layer (ONL) thickness of retinas injected with mutant IMPDH1 is much less than those injected with WT IMPDH1 and uninjected IMPDH1$^{+/-}$ retinas. RPE, retinal pigment epithelium; ONL, outer nuclear layer; OS, outer segment; ONL, outer nuclear layer; OPL, outer plexiform layer; INL, inner nuclear layer; IPL, inner plexiform layer; GCL, ganglion cell layer. Scale bar: 40 μm.

severely degenerated with complete absence of OS and reduction of number of rows of photoreceptor nuclei in the ONL to zero (Fig. 6B). In stark contrast the entire retinal structure including the photoreceptor layer appeared wholly normal in the left eye which received AAV-WtIMPDH1 (Fig. 6B). Real-time RT–PCR analysis showed that the level of AAV-mediated IMPDH1 expression on an IMPDH1 null background was equivalent to the WT levels (data not shown).

To assess whether suppression of mutant IMPDH1 by AAV-sh2048 *in vivo* could rescue the photoreceptors from degeneration in this AAV-induced model, 18 adult WT 129 mice were sub-retinally co-injected at an approximate viral particle (vp) ratio of 1 AAV-cDNA: 5 AAV-shRNA as follows; (i) 1 μl of AAV-EGFP (1×10^{12} vp/ml) and 2 μl of AAV-sh2048 (3.3×10^{12} vp/ml; right eye) or AAV-shLuc (3.3×10^{12} vp/ml; left eye) ($n = 5$); (ii) 1 μl of AAV-WtIMPDH1.EGFP (1.77×10^{12} vp/ml) and 2 μl of AAV-sh2048 (3.3×10^{12} vp/ml) or AAV-shLuc (3.3×10^{12} vp/ml; left eye) ($n = 5$); (iii) 1 μl of AAV-Mut224IMPDH1 (1.4×10^{12} vp/ml) and 2 μl of AAV-sh2048 (3.3×10^{12} vp/ml; right eye) or AAV-shLuc (3.3×10^{12} vp/ml; left eye) ($n = 8$). Four weeks post-injection, all animals were sacrificed and retinal sections were visualized by confocal microscopy. Eyes treated with either AAV-EGFP or AAV-WtIMPDH1 virus and either shRNA virus showed similar retinal structures to those observed in uninjected animals (data not shown). However, representative fluorescent images from the left eyes of eight mice co-injected with AAV-Mut224IMPDH1 and AAV-shLuc showed significant deterioration in ONL thickness (Fig. 7A), which was consistent with those previously injected with AAV-Mut224IMPDH1 vector alone (Fig. 6B). In contrast, the contralateral eyes of these mice treated with AAV-Mut224IMPDH1 and AAV-sh2048 displayed a robust ONL indicating that AAV-sh2048 provided significant protection of the ONL from rapid degeneration (Fig. 7A). The average positively transduced ONL area per unit length in the left eyes of these animals were then compared with that of the right eyes, and on average, all eight animals showed a significant increase in ONL area per unit length in eyes co-injected with AAV-Mut224IMPDH1 and AAV-sh2048 (35.53 ± 1.49 μm), compared with AAV-Mut224IMPDH1 and AAV-shLuc controls (15.50 ± 0.68 μm) ($P < 0.05$; Fig. 7B).

Off-target effects against IMPDH2

Understanding off-target effects is not only important for siRNA design, but is also crucial for the development of siRNAs as therapeutic tools. Since IMPDH1 and IMPDH2 proteins share 84% homology (5,9), it is plausible that siRNA targeting IMPDH1 might exhibit off-target effects on IMPDH2 even though the sequences of si1224 and si2048 were specifically selected because they contained mismatches against IMPDH2. To investigate this possibility, HeLa cells were separately transfected with si1224 or si2048 and the level of endogenous IMPDH2 transcripts was measured 24 h post-transfection by quantitative real-time RT–PCR. IMPDH2 expression was standardized per unit β-actin

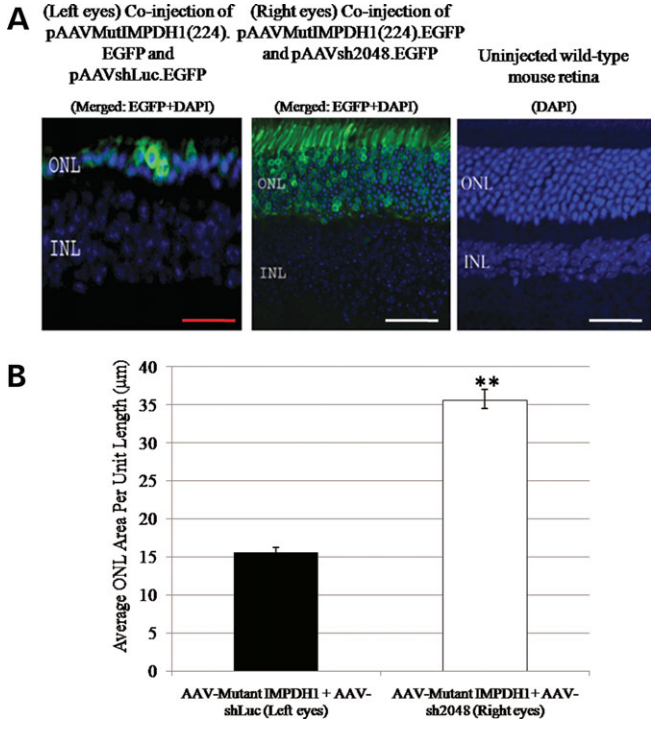

Figure 7. Protection of photoreceptor cells from deterioration by shRNA-mediated suppression of mutant IMPDH1 *in vivo*. (**A**) Histological analysis of WT 129 mouse retinas co-injected with AAV-mutant IMPDH1 and AAV-shLuc (left panel), AAV-mutant IMPDH1 with AAV-sh2048 (middle panel) and uninjected retina (right panel). rAAV-sh2048-mediated suppression of mutant IMPDH1 protects the ONL from degeneration to an extent to that observed in the WT uninjected retina. White scale bar: 40 μm. Red scale bar: 20 μm. (**B**) Histograms illustrating average ONL area per unit length (μm) of positively transduced areas in eyes co-injected with AAV-mutant IMPDH1 and AAV-shLuc or AAV-sh2048. $^{**}P \leq 0.0001$ ($n = 8$). Y-error bars denote standard error of the mean.

expression and expressed as a percentage of that for the siLuc control. HeLa cells treated with si1224 and si2048 showed non-significant reduction of IMPDH2 mRNA to 90 ± 9.5 and $89 \pm 7.21\%$, respectively, when compared with the control ($P = 0.7681$ and $P = 0.7372$, respectively; Fig. 8A). Thus, both IMPDH1-specific siRNAs show, at most, a very limited trend for off-target effects against IMPDH2 at the mRNA level.

However, in order to investigate the possibility that mismatches between IMPDH1-specific shRNAs and IMPDH2 coding region might provoke a microRNA (miRNA) response by inducing translational blockade which would be undetectable by real-time RT–PCR, HeLa cells were separately co-transfected with 1 μg/μl pWtIMPDH2 and psh1224 or psh2048 and expression levels of IMPDH2 analysed by western blot analysis 72 h later using anti-N-IMPDH2 antibody. Consistent with quantitative real-time RT–PCR data, HeLa cells co-transfected with sh1224 or sh2048 showed no significant reduction of IMPDH2 protein (lanes 1 and 2; Fig. 8B), compared with the luciferase-targeting control (lane 3; Fig. 8B). In particular, average densitometric measurements taken from two independent experiments showed no significant changes of IMPDH2 expression at the protein level by sh1224 ($90 \pm 13\%$) and sh2048 ($101 \pm 5\%$), compared with the shLuc control ($P = 0.43$ and $P = 0.86$, respectively). Endogenous mouse IMPDH2 protein expression was also detected in WT 129 mouse retinal extracts using anti-N-IMPDH2 antibody as shown in Figure 8C. In addition, retinal protein extracts used to demonstrate IMPDH1 suppression (Fig. 5C) were subjected to western blot analysis for the detection of IMPDH2 using anti-N-IMPDH2 antibody. In contrast to IMPDH1, no changes in the levels of IMPDH2 protein were detected between retinas injected with AAV-sh2048 and the non-targeting AAV-shLuc as shown in lanes 1 and 2 of Figure 8D. Densitometric analysis confirmed the observation that AAV-sh2048 did not significantly affect IMPDH2 expression, which remained at $95 \pm 5\%$ compared with the control ($P = 0.82$). Thus, the absence of significant silencing of IMPDH2 at the protein level further illustrates the specificity of both IMPDH1-specific shRNAs in mammalian cells and *in vivo*, and also provides strong evidence that mismatches between IMPDH1-specific shRNAs and IMPDH2 do not give rise to a miRNA-related protein translational inhibitory response.

DISCUSSION

Previous investigations into the molecular pathology of RP10 (12), together with studies on the autosomal recessive form of disease in the IMPDH1$^{-/-}$ mouse, have suggested that simultaneous suppression of normal and mutant IMPDH1 alleles might be sufficient to abolish the dominant negative effect exerted by the mutant protein, and perhaps prolong the survival of photoreceptor neurons. The therapeutic potential of RNAi in treating adRP has been described in a number of recent publications. For example, Tessitore *et al*. (27) used AAV-mediated expression of shRNA targeting murine rhodopsin in a rat model of adRP caused by the heterozygous expression of a murine Pro23His rhodopsin mutation, although retinal histopathology was not rescued, the authors arguing that more robust expression of shRNA would be required. Gorbatyuk *et al*. (28) demonstrated *in vivo* suppression of rhodopsin following sub-retinal delivery of rAAV-2/5 vectors expressing shRNA directed against murine rhodopsin transcripts in heterozygous RHO$^{+/-}$ mice. Moreover, O'Reilly *et al*. (23) showed that sub-retinal delivery of rAAV-2/5 vectors expressing a codon-modified rhodopsin replacement gene in the presence of rhodopsin-targeting shRNAs significantly protected the ONL of the retina in a murine model of retinal degeneration.

In this study, we have addressed the concept of developing an RNAi-mediated therapy for the RP10 form of adRP, a condition selected not only in view of its prevalence, but because features of the molecular pathology of the disease render it particularly suited to the development of such a therapy. Specifically, expression of a rod-opsin promoter-driven WT IMPDH1 gene in retinal tissues appears to have no detrimental pathological effect, and secondly, mice with a targeted disruption of the IMPDH1 gene develop only an exceedingly mild retinopathy (12). Taken together, these observations suggest that suppression of IMPDH1 by an RNAi-based gene therapy, may on its own, have a substantially ameliorating

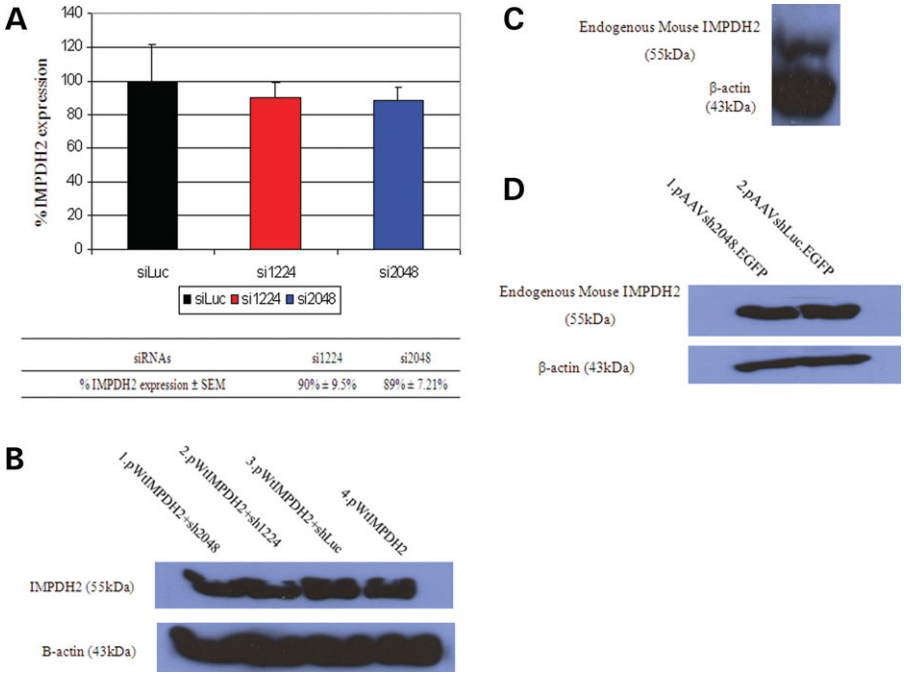

Figure 8. Off-target silencing of IMPDH2 *in vitro* and *in vivo*. (**A**) Off-target silencing of IMPDH2 mRNA by IMPDH1-specific siRNAs in HeLa cells. Percentage IMPDH2 expression was determined by real-time RT–PCR 24 h post-transfection and normalized to the house-keeping gene, β-actin. The average of five experiments is shown; Y-error bars denote standard error of the mean. $^{*}P < 0.05$. (**B**) shRNA-mediated down-regulation of IMPDH2 protein expression in HeLa cells. HeLa cells were separately co-transfected with pWtIMPDH2 and psh1224 or psh2048. Protein was extracted 72 h post-transfection and analysed by western blotting using anti-N-IMPDH2 antibody. (**C**) Detection of endogenous mouse IMPDH2 protein in WT C57B6/CBA mouse retinas. (**D**) AAV-shRNA-mediated suppression of IMPDH2 protein expression in WT mice.

potential and moreover, should a replacement therapeutic IMPDH1 gene, engineered to be resistant to the suppressive effect of RNAi be required, precise control of expression levels may not be as crucial as in other systems, such as diseases based on mutations within the rhodopsin or RDS-peripherin genes, where it has been shown that under- or over-expression of normal genes can be pathogenic to the retina (29–32).

We have successfully shown that shRNAs can be used to suppress both human and mouse IMPDH1 expression *in vitro*, *ex vivo* and *in vivo*. The most potent siRNA tested, si2048, selectively suppressed IMPDH1 expression by >70% at both the mRNA and protein level in HeLa cells in a mutation-independent manner, without, importantly, decreasing levels of IMPDH2 transcript or protein. In order to secure longer-term silencing, si2048 was cloned into a H1-driven RNAi vector, which also resulted in potent silencing of IMPDH1 in cell cultures. The efficacy of RNAi-mediated silencing is highly dependent on the endogenous RNAi pathway, which may vary between *in vitro* and *in vivo* systems. Therefore the robustness of sh2048 was further tested in murine retinal explants, which provided a cellular environment similar to that of retinal tissues. The construction of a dual expression RNAi vector system and FACS analysis provided a rapid and sensitive method for sorting positively transfected retinal cells, which allowed evaluation of shRNA-mediated silencing of IMPDH1 in a true transfectant population. *In vitro* electroporation of sh2048 showed long-term and stable suppression of IMPDH1 by >80% *ex vivo* in retinal explants. In addition, *in vitro* electroporation of sh2048 did not cause any observable damage to the cultured retinas, where the histology resembled that of a normal retina *in vivo*, with defined retinal morphological differentiation (Fig. 4D).

For adRP, the ability to achieve persistent shRNA expression from a viral vector is highly desirable, especially when long-term and stable suppression of mutant protein is required to obtain therapeutic benefits (23,28). In order to secure long-term expression of shRNAs in living retinas in mice, AAV was used as the vector of choice, in view of its record of safety and non-pathogenic characteristics *in vivo* (33–35). Previous reports have documented safe and prolonged expression of rAAV-mediated delivery of therapeutic transgenes in mouse and canine models of retinal diseases (36–38). Sub-retinal delivery of rAAV-2/5 vectors expressing IMPDH1-specific shRNA and EGFP exclusively transduced the RPE, OS and ONL of WT mouse retinas when analysed 4 weeks post-injection, which is consistent with the transduction pattern previously reported by O'Reilly *et al.* (23) and Aurrichio *et al.* (26). Immunolocalization studies have shown that IMPDH1 is predominantly localized in the OS, and outer and inner nuclear layer (Fig. 5D), which is consistent with the *in situ* mRNA expression pattern previously reported by Aherne *et al.* (12), and with the immunohistochemical study reported by Bowne *et al.* (15). The presence of IMPDH1 predominantly in the photoreceptor cell layers is not surprising as IMPDH1 is largely responsible for the production of guanine nucleotides within photoreceptor cells

(12,15). This observation also offers a plausible reason as to why mutations in IMPDH1 exclusively affect photoreceptor cells. Real-time RT–PCR analysis of pure transfectant populations obtained following FACS analysis showed that rAAV-sh2048 mediated significant knockdown of endogenous IMPDH1 transcripts by up to 70% in the ONL of WT mice. In addition, FACS analyses indicated that a single sub-retinal injection of rAAV-2/5 viral vectors expressing EGFP was capable of transducing up to 50% of total retinal cells (data not shown). Western blot analyses showed that rAAV-sh2048 significantly suppressed endogenous IMPDH1 protein expression in WT C57B6/CBA mice following two sequential sub-retinal injections. Lotery *et al*. (39) previously demonstrated the use of controlled multiple sub-retinal injections to allow widespread transduction of non-human primate retinas and showed that this method reduced surgical trauma to the overall retinal structure. Immunohistochemical analysis also showed that rAAV-sh2048 specifically suppressed endogenous IMPDH1 protein expression in the OS and ONL of WT mice. Furthermore, no significant damage to the overall retinal structure was detected following 4 weeks of rAAV-mediated expression of shRNA *in vivo*.

rAAV-mediated expression of human mutant IMPDH1 harbouring the Arg224Pro mutation, but not WT IMPDH1, in the ONL of IMPDH1$^{+/-}$ (Fig. 6) and WT (Fig. 7a) mice, has been shown to produce rapid structural and functional retinal degeneration similar to that observed in transgenic mice bearing the P23H rhodopsin mutation (40). Similarly, Cashman *et al*. (41) have shown that adenovirus-mediated sub-retinal delivery of human *VEGF165* [a major stimulant of choroidal neovascularization (CNV)] into murine retinas induces a retinopathy with properties resembling that of the exudative form of AMD. In particular, the authors showed that CNV could be rapidly induced within 5 days following sub-retinal injection. Although the pathological effect induced by expression of mutant IMPDH1 has not yet been fully deciphered in the retina, previous studies have shown that mutant IMPDH1 protein is likely to cause protein aggregation *in vitro* through significant disruption to its protein structure (12). Photoreceptor degeneration caused by protein aggregation has previously been reported in other adRP-linked mutations, such as the Pro23His mutation in rhodopsin (42), and the R14W mutation in the gene encoding carbonic anhydrase IV that causes RP17 (43). In addition, protein aggregation caused by polyglutamine expansion has been identified as the underlying disease mechanism for several neurological disorders such as Huntington's disease and spinocerebellar ataxia (44–46). In the current context, persistent rAAV-mediated expression of human mutant IMPDH1 in the retinas of WT mice has provided a rapid retinal degenerative model for RP10 that could be established within 4 weeks post-injection. Notably, simultaneous sub-retinal delivery of rAAV-mutant IMPDH1 harbouring the Arg224Pro mutation, together with rAAV-sh2048 in WT mice, provided significant therapeutic protection of photoreceptor cell layer from degeneration, when compared with controls in which mutant IMPDH1 together with a non-targeting shRNA molecule were expressed. These observations provide a proof-of-concept for down-regulation of mutant IMPDH1 as a therapeutic strategy for RP10.

The co-existence of two IMPDH iso-enzymes in mammalian cells with striking similarities in both their amino acid identity and kinetic parameters suggests that each subserves an important and non-overlapping function in cellular physiology and development (5–7). Regulation of IMPDH activities during cellular transformation and differentiation has mainly been attributed to specific changes in the expression of IMPDH2 mRNA, whereas IMPDH1 remains constitutively expressed (11). Expression studies have also revealed that human IMPDH2 is regulated by a single core promoter region (47), whereas expression of human IMPDH1 is governed by three separate transcription initiation sites, which suggests a cell type-specific expression pattern (48). In regard to further optimizing the current approach to therapy for RP10, it is worth noting that target recognition by siRNA was initially thought to be a highly sequence-specific gene silencing mechanism where by a single mismatch between the guide strand of siRNA and target mRNA was sufficient to terminate gene silencing. However, a growing body of evidence has indicated that siRNA specificity is not guaranteed and non-specific silencing can occur through various mechanisms such as; (i) global up- or down-regulation of genes using high dosages of siRNA (49,50); (ii) the induction of interferon response (51); (iii) miRNA-like translational inhibition (52–54) and (iv) mRNA degradation by partial sequence complementation (55). Previous reports have shown that miRNA-mediated translational repression commonly occur through partial complementarity to a site in the 3′-untranslated region of targeted transcripts (56,57). However, a previous study has shown that a natural miRNA that is partially complementary to the coding region of a target mRNA led to translational repression in mammalian cells (58). Furthermore, Saxena *et al*. (53) demonstrated that siRNAs bearing mismatches to the coding region of an endogenous target mRNA in HeLa cells caused a significant decrease at the protein level, but not at the transcript level. These observations have prompted further studies to examine whether IMPDH1-specific siRNAs bearing mismatches to the coding region of IMPDH2 would elicit miRNA-related translational inhibitory response. IMPDH2 was a good candidate for the study of non-specific silencing effects in this particular study because of its close sequence homology to IMPDH1 in terms of both the amino acid identity and enzymatic properties (5–9). In our current study, *in vitro* and *in vivo* analyses have indicated that both of the IMPDH1-specific siRNAs exhibited minimal silencing effects on IMPDH2 expression at the mRNA and protein level. This specificity may have been permitted by the presence of nucleotide mismatches located between the seed region (equivalent to nucleotide positions 2 to 8) of the antisense strands and the target sequence (Fig. 1A). A previous study demonstrated that the seed region of siRNA antisense strand represents a low-tolerance region, implying that mismatches at these positions with the target sequence significantly abolish most of the suppression activity (59). Furthermore, partial complementarity between IMPDH1-specific shRNAs and IMPDH2 did not lead to miRNA-mediated translational repression *in vitro* or *in vivo*. Results of two separate studies have previously illustrated that miRNAs with high G/C content at positions 2 to 8 of the

antisense strand induce a high thermodynamic stability in the 5′ region of the miRNA antisense strand, which may cause translational inhibition of targets without requiring extensive complementation at the 3′ region of the antisense strand (60,61). This may explain the lack of miRNA-mediated translational repression observed on IMPDH2 as both IMPDH1-specific shRNAs possess low G/C contents (≥30%) in positions 2 to 8 in the 5′ region of their antisense strands.

Collectively, the results obtained in this study show that both human WT and mutant IMPDH1 genes can be markedly suppressed by shRNA *in vitro*, *ex vivo* and *in vivo*. In particular, the proof-of principle of rAAV-mediated gene therapy in the mutant IMPDH1-induced RP10 mouse model, in conjunction with accumulating evidence that rAAV represents a safe and efficient means of delivering molecular therapies to the retina (62), suggest that the current rAAV-mediated RNAi suppression strategy holds substantial promise for the development of future therapies for RP10 patients. However, a number of issues regarding the safety of rAAV-mediated retinal gene transfer will need to be addressed. First, genome-wide gene expression profiling will be required to provide a comprehensive picture of any possible off-target effects elicited by sh2048. In addition to the importance of possible changes at the transcriptional level, it is imperative to profile retinal miRNAs following the inoculation of rAAV-shRNAs, since it has been reported that excessive RNAi can cause lethality in mice by oversaturation of the natural endogenous RNAi/miRNA pathway (63). In this regard, a novel approach for safer RNAi by sub-cloning shRNAs sequences into the backbone of naturally occurring miRNAs, in order to address the concerns over obstructing the natural endogenous RNAi machinery (64,65), may provide a safer long-term application of shRNA expression *in vivo*. In summary, we show that shRNA-mediated suppression of mutant human IMPDH1 transcripts provides significant therapeutic benefit at a point where all photoreceptors are normally destroyed in an AAV-induced model of RP10. These data provide a solid basis for the further development of a gene-based therapy for the RP10 form of RP in man. Detailed evaluation of phenotypic effects of long-term expression of shRNA and of elevated expression of a normal human IMPDH1 gene (readily modifiable such as to be resistant to RNAi-mediated suppression) in the non-human primate retina will hopefully facilitate translation to human subjects within a realistic time-frame.

MATERIALS AND METHODS

Construction of IMPDH1 and IMPDH2 expression plasmids

The generation of IMPDH1 vectors has previously been described by Aherne *et al*. (12). The 1.5-kb WT human IMPDH1 cDNA insert was cloned into the *Xho*I site of the pcDNA3.1(+) vector (Invitrogen) to produce pWtIMPDH1. The single point-mutations CGC to CCC (Arg224Pro) and GAC to AAC (Asp226Asn) were introduced into the WT human IMPDH1 cDNA, as described previously by Aherne *et al*. (12), and cloned into the *Xho*I site of pcDNA3.1(+) to generate pMutIMPDH1(224) and pMutIMPDH1(226), respectively. Primers were designed to introduce *Not*I site at the 5′ end, and an *Xho*I site at the 3′ end of the WT human IMPDH2 cDNA sequence in the pET-30 Ek/LIC+IMPDH2 vector (Dr Sara Bowne, University of Texas HSC, USA). The 1.5 kb IMPDH2 cDNA was amplified using *Pfu* DNA polymerase (Stratagene) and inserted in-frame into the respective restriction sites in pcDNA3.1(+), to create pWtIMPDH2. In order to generate EGFP reporter plasmids, the EGFP gene (630 bp) was first excised from pEGFP-N1 (Clontech, BD Biosciences, Inc.), and inserted in between the *Hin*DIII and *Not*I sites of pWtIMPDH1, pWtIMPDH2, pMutIMPDH1(224) and pMutIMPDH1(226), which was upstream of the IMPDH1 and IMPDH2 cDNAs, creating pWtIMPDH1.EGFP, pWtIMPDH2.EGFP, pMutIMPDH1(224).EGFP and pMutIMPDH1(226).EGFP, respectively. The sequences of all IMPDH1 and IMPDH2 plasmids were verified by DNA sequencing using ABI 310 Genetic Analyser (Perkin Elmer, Shelton, CT, USA).

Design of IMPDH1-specific siRNAs and shRNAs

The selection of IMPDH1 target sequences was determined by submitting the human IMPDH1 sequence (GenBank accession no. NM_000883) to the search-engine supplied by www.dharmacon.com. The resulting sequences were then filtered using the 8-criterion algorithm method (17) to select optimal siRNAs. Two siRNA sequences denoted as si1224 and si2048 (Table 1), targeting distinct regions on human IMPDH1 transcript were selected. The siRNAs were synthesized by Dharmacon, resuspended to a final concentration of 20 pmol in RNase-free water (Promega). Both IMPDH1-targeting siRNAs were generated as oligonucleotides and sub-cloned into the pBluescript-H1 vector system to create psh1224 and psh2048 (66) (Table 1), respectively, as outlined in the protocol provided by www.oligoengine.com (Oligoengine). A commercial synthetic siRNA duplex targeting luciferaseGL3 (siLuc) was used as a non-targeting siRNA control (Table 1). An additional siRNA duplex targeting luciferaseGL2 (Qiagen) was generated as oligonucleotides and sub-cloned into pBluescript-H1 vector system to create pshLuc as outlined in the protocol provided by www.oligoengine.com (Oligoengine). To generate dual expression shRNA plasmids, restriction fragments containing the H1-promoter, shRNA sequences and termination signal were excised from pshLuc and psh2048, respectively, by restriction enzyme digestion at *Eco*RI and *Hin*dIII. The fragments were then sub-cloned into pEGFP-1 (Clontech) into which the CMV promoter (PCR amplified from pcDNA3.1+) had been inserted immediately 5′ of the EGFP cDNA, to give pshLuc.EGFP and psh2048.EGFP, respectively. A 300 bp Ubc intron was PCR amplified from pUB6/V5-His A, B, C (Invitrogen) and inserted in between the H1 and CMV promoters (22). Correct insertions of shRNA oligonucleotides were verified by DNA sequencing using ABI 310 Genetic Analyser (Perkin Elmer).

Cell culture and transfection of siRNAs

HeLa (ATCC number: CCL-2) cells were cultured in Dulbecco's modified Eagle medium (DMEM, Gibco-BRL) supplemented with 10% fetal calf serum (FCS), 1%

L-glutamine (2 mM), sodium pyruvate (2 mM) and 1% streptomycin/penicillin, in a 5% CO_2 incubator at 37°C. Cultured cells were passaged regularly with trypsin–EDTA (Gibco-BRL) to maintain exponential growth. Twenty-four hours prior to transfection, HeLa cells were trypsinized, diluted in DMEM without antibiotics at 1×10^5 cells/ml, and plated onto 24-well plates (500 μl per well). To evaluate siRNA and shRNA *in vitro*, 1 μg/μl of pBluescriptH1 expressing IMPDH1-shRNAs or 20 pmol chemically synthesized siRNAs were diluted in Opti-MEM I (Gibco-BRL) and transfected into HeLa cells using Lipofectamine 2000® according to manufacturer's protocol (Invitrogen). Each sample was carried out in quadruplicates and pooled together during RNA extraction.

Generation of AVVs

AAV were prepared as previously described (23). Genomic titres, i.e. vp (vp/ml) were determined by quantitative real-time RT–PCR according to the method described by Rohr *et al*. (67). The IMPDH1 suppressor and non-targeting shRNAs were sub-cloned into pAAV-MCS (Stratagene) to generate pAAV-sh2048.EGFP and pAAV-shLuc.EGFP, respectively (Fig. 4A). pAAV-CMV.EGFP; EGFP was excised from pEGFP-1 (Clontech), and blunt cloned into pAAV-MCS. The CMV promoter in pAAV-IRES-EGFP was replaced with 1.7 kb mouse rhodopsin promoter [excised from the 17.1 kb mouse rhodopsin genomic clone (29)] to create pAAV-Rho-IRES-EGFP, and both WT and mutant IMPDH1 cDNAs were sub-cloned into pAAV-Rho-IRES-EGFP, to create pAAVWtIMPDH1.EGFP and pAAV-Mut224IMPDH1.EGFP, respectively.

Total RNA isolation for quantitative real-time RT–PCR analysis of IMPDH1 mRNA

Twenty-four hours post-transfection, total RNA was extracted from cultured cells using TRIzol reagent (MRC) according to manufacturer's protocol. RNA was quantified using real-time RT–PCR on a Light-Cycler system (Roche Diagnosis) with Quantitect SYBR Green Kit according to manufacturer's protocol (Qiagen Xeragon). The following reaction conditions were used for real-time RT–PCR: 50°C for 20 min; 95°C for 15 min; 35 cycles of 95°C for 15 s; 57°C for 20 s; 72°C for 8 s; 95–65°C for 10 s and 40°C for 30 s. Complementary HPLC-purified primers (Sigma-Genosys) for amplifying DNA sequences are provided in (Table 2). For *in vitro*, *ex vivo* and *in vivo* experiments, the level of IMPDH1 mRNA was standardized to the housekeeping gene, β-actin, although other housekeeping genes such as human IMPDH2 (GenBank accession no. NM_000884) and human transcription binding protein (TBP) (GenBank accession no. NM_003194) were also tested and yielded similar results (data not shown). For each transfection experiment, a control group was transfected with a non-targeting siRNA/shRNA, and IMPDH1 was standardized per unit β-actin expression and expressed as a percentage for the non-targeting control.

Murine retinal explants

In vitro *electroporation*. Electroporation and maintenance of retinal explant cultures were carried out according to protocols previously described by Kiang *et al*. (21) and Palfi *et al*. (22). A total of 12 retinas were dissected from 6 new born C57B6/CBA mouse pups and transferred to a micro-electroporation chamber (Nepagene, 3 × 10 × 5 mm) filled with 100 μl of pshLuc.EGFP or psh2048.EGFP at a final concentration of 1 μg/μl in Hank's balanced salt solution (HBSS). Five square pulses (30 V) of 50-ms duration with 950-ms intervals were applied to the retinal tissues from the scleral side using a pulse generator (ECM 830 BTX). Electroporated retinas were cultured *in vitro* at 37°C on Costar Transwell polycarbonate membrane (0.2 μm pore) in neurobasal medium (Invitrogen) containing 2 mM taurine, 10% FCS, penicillin/streptomycin and B-27 supplements (Invitrogen) for 14 days.

Fluorescent activated cell sorting. Neurobasal media were discarded latter to *in vitro* culturing and retinal tissues were washed twice with 4 ml HBSS solution for 1 min. For cell sorting, six cultured retinal explants per construct per experiment were pooled together and dissociated into single cells by digestion with 2 ml of trypsin (1 mg/ml) (Roche) at 37°C for 20 min. Two to three microlitres of DNaseI was added to the dissociated cells and was further incubated at 37°C for 10 min. Two-hundred nanolitres of trypsin inhibitor (Roche) was added to the cell suspension and centrifuged for 5 min at 1200 rpm (IEC micromax microcentrifuge, Thermo Electron Corporation). The pellet was then resuspended in 2 ml HBSS solution per pair of retinas. Ten microlitres of DNaseI was added to the cell suspension and incubated at 37°C for 10 min. Dissociated retinal cell suspensions (six retinas pooled together) were then sieved through 50 μm Filcon filters (Dakocytomation). EGFP-positive and EGFP-negative cells were collected in a Beckman-Coulter Altra Fluorescence Activated Cell Sorter (Beckman-Coulter, Inc., Fullerton, CA, USA) at a rate of 1000 cells/s. Approximately 100 000–540 000 EGFP-positive cells per experiment were collected. The FACS sorter was incorporated with three lasers at 488 nm (blue), 633 nm (red) and 407 nm (violet) that enabled detection of two scattered signals. The sorting flow rate of 4 was used to maximize the purity of the final sample. Subsequent to FACS sorting, the isolated cells were concentrated through 0.45 μm Ultrafree-MC filter units (Amicon, PTFE membrane) by centrifuging at 1300 rpm for 1 min at a concentration of $\leq$200 000 cells/unit, and eluted by adding 350 μl RNA lysis buffer (RNeasy Mini Kit, Qiagen). For real-time RT–PCR analysis, RNA was extracted and purified from FACS-sorted cells using the RNeasy Mini Kit (Qiagen) according to manufacturer's protocol.

For *in vivo* studies, 2 weeks to 1-month-old WT C57B6/CBA mice were sub-retinally injected with 1–3 μl of 10^{12-13} vp/ml pAAVshLuc.EGFP (left eyes) and pAAVsh2048.EGFP (right eyes). Four weeks post-injection, AAV-transduced retinas were dissected, pooled and dissociated by trypsin digestion. Dissociated single retinal cells expressing EGFP were FACS-sorted and RNA was extracted from EGFP-positive cells for real-time RT–PCR analysis as described above.

Table 2. Sequences of HPLC-purified primers for real-time RT–PCR amplification

Gene		GenBank Accession number	Sequences (5′→3′)	Product size (bp)
Human and mouse IMPDH1	Forward	NM_000883 (Human)	5′-cgtgaggatgacaaataccg-3′	99
	Reverse	RC053416 (Mouse)	5′-accatggcgatctgatacac-3′	
Human and mouse IMPDH2	Forward	NM_000884 (Human)	5′-acacctgaattccaggccaa-3′	193
	Reverse	BC052671 (Mouse)	5′-gaggagatgatgcccaccaa-3′	
Human and mouse β-actin	Forward	XM004814 (Human)	5′-tcacccacactgtgcccatctacga-3′	296
	Reverse	EF095208 (Mouse)	5′-cagcggaaccgctcattgccaatgg-3′	
Human TBP	Forward	NM_003194	5′-gcatattttcttgctgccagtct-3′	90
	Reverse		5′-accacggcactgattttcagtt-3′	

Histological and immunohistochemical analysis

Whole eyes were extracted from injected mice and immediately fixed in 4% paraformaldehyde (pH 7.4) for 4 h at 4°C on a rotating device. Eye cups were then washed in phosphate-buffer saline (PBS) for 1 hr and sequentially submerged in 10, 20 and 30% sucrose. Eye cups were then suspended in specimen blocks with OCT solution (Tissue Tek) and snap frozen using liquid nitrogen. Frozen eyes were cryo-sectioned on a cryo-sectioner (Leica CM 1900) in 12 μm thickness and sections were collected on Polysine® slides (Menzel-Glazer). To detect IMPDH1, sectioned retinas were blocked for 20 min at room temperature in PBS containing 5% goat serum, and immunostained with anti-C-IMPDH1 antibody (15) over-night at 4°C in a humidity chamber. Sectioned retinas were then washed three times with PBS at 15 min intervals, and incubated in Cy3-labelled anti-rabbit IgG antibody for 1 hr at 37°C in a humidity chamber. Following incubation, sectioned eyes were washed six times with PBS at 15 min intervals and mounted with Aqua-Polymount (Polyscience) mounting medium after nuclei-counterstaining with DAPI (1:5000 in PBS). Retinal sections were then visualized under fluorescent microscope (Zeiss, Axioplan 2) and confocal microscope (Olympus FU1000, Hamburg, Germany).

Electroretinography

Animals were dark-adapted overnight and prepared for electroretinography under dim red light. Pupillary dilation was carried out by installation of 1% cyclopentalate and 2.5% phenylephrine. Animals were anesthetized by intraperitoneal injection with ketamine (2.08 mg per 15 g body weight) and xylazine (0.21 mg per 15 g body weight). Standardized flashes of light were presented to the mouse in a Ganzfeld bowl to ensure uniform retinal illumination. The ERG responses were recorded simultaneously from both eyes by means of gold wire electrodes (Roland Consulting Gmbh) using 1% Amethocaine as topical anaesthesia and Vidisic (Dr Mann Pharma, Germany) as a conducting agent and to maintain corneal hydration. Reference and ground electrodes were positioned subcutaneously, ∼1 mm from the temporal canthus and anterior to the tail respectively. Responses were analysed using a RetiScan RetiPort electrophysiology unit (Rolad Consulting Gmbh). The protocol was based on that approved by the International Clinical Standards Committee for human electroretinography. Rod-isolated responses were recorded using a dim white flash (−25 dB maximal intensity where maximal flash intensity was 3 candelas/m^2/s) presented in the dark-adapted state. Maximal combined rod-cone response to the maximal intensity flash was then recorded. a-waves were measured form the baseline to the trough and b-waves from the baseline (in the case of rod-isolated responses) or from the a-wave to the trough (12,23). All ERG analyses were carried out by a registered ophthalmologist (Dr Paul F. Kenna) in a barrier facility with sterile instruments and solutions.

Evaluation of photoreceptor cell morphology by quantitative histology

After ERG recordings, injected mice were sacrificed and the eyes were cut at 12 μm thickness on a cryo-sectioner (Leica CM 1900) as above. Eyes were cut along the vertical meridian, such that the superior and inferior hemispheres were separated by the optic nerve. To evaluate quantitatively the area per unit length and thickness of positively transduced ONL, 12 μm frozen sections were viewed under a fluorescent microscope (Zeiss, Axioplan 2). EGFP-positive ONLs from nine independent frozen sections from each animal co-injected with AAV-mutant IMPDH1 and AAV-sh2048 or shLuc were measured using analytical software tools (Analysis B, Zeiss), and the average area per unit length for each co-injected animals was grouped. The mean positively transduced ONL area per unit length was compared to control eyes.

Western blot analysis

Twenty-four hours prior to transfection, HeLa cells were plated at a density of 3×10^5 cells/ml onto 6-well plates with DMEM medium without antibiotics (2 ml per well). Separate wells of HeLa cells at a confluency of 80–90% confluency were then co-transfected with 1.5 μg/μl IMPDH1-expression plasmids with 100 pmol siRNAs or 1 μg/μl shRNAs diluted in Opti-MEM-reduced serum medium using Lipofectamine 2000® according to manufacturer's protocol. For *in vivo* studies, adult WT C57B6/CBA mice were sub-retinally injected with 3 μl of 10^{12-13} vp/ml pAAVshLuc.EGFP (left eyes) and pAAVsh2048.EGFP (right eyes) per eye. A second sub-retinal injection with the same concentrations of AAV shRNAs was administered into the same eyes at different regions of the retina 1 week after the primary injection. Four weeks after the second injection, mice were euthanized by carbon dioxide inhalation, and retinas were dissected. Protein extracts were obtained from cultured cells and dissected retinas by passing through

21-gauge syringes in protein lysis buffer. Protein concentration was determined by BCA Protein assay kit (Pierce) with bovine serum albumin (BSA) at 2 mg/ml as standards on 96-well plates according to manufacturer's guidelines. 30 μg of total protein was loaded in each lane. Protein samples were separated by electrophoresis on 10% SDS-polyacrylamide gels under reducing conditions, and transferred to nitrocellulose membranes. Membranes were incubated overnight in blocking buffer, and probed with anti-N-IMPDH1 and anti-N-IMPDH2 antibodies (15) overnight at 4°C. Detection of primary antibody complexes was carried out using horse-radish conjugated secondary antibodies (Abcam). Each blot was stripped using Stripping solution (Pierce) and immunostained with β-actin antibody (Abcam) as loading controls. The blots were developed using Enhanced Chemiluminescent Kit (Pierce Chemical Co.) and exposed to Fugi X-ray films in a dark-room facility. Protein band intensities were quantified by scanning with Epson Stylus CX3200 and analysed using Multi Gauge Analysis Software (Ver. 2.2, Fujifilm). The percentage reduction in band intensities of IMPDH1 was calculated relative to the non-targeting control, which was standardized to represent 100% IMPDH1 expression and normalized against β-actin.

Animals and sub-retinal injection

The use of animals and sub-retinal injections carried out in this work were in accordance with the European Communities Regulations 2002 and 2005 (Cruelty of Animals Act) and the Association for Research in Vision and Ophthalmology statement for the use of Animals in Ophthalmic and Vision Research and were approved by the institutional Ethics Committee. C57B6/CBA (Harlan, UK) and 129 S2/SvHsd (Harlan, UK) mice were bred and maintained in a 12 hour light-dark cycle. A registered ophthalmologist (Dr Paul F. Kenna) performed all procedures in a barrier facility with sterile instruments and solutions. In brief, 2 weeks to 4 months old mice were anesthetized by intraperitoneal injection of Medetomidine and Ketamine (10 and 750 μg/10 g body weight, respectively). Pupils were dilated with 1% cyclopentolate and 2.5% phenylephrine, and, under local analgesia (Amethocaine), a small puncture was administered in the sclera. Under microscopic control, a 34-gauge blunt-ended micro-needle attached to a 10 μl syringe (Hamilton, Bonaduz, Switzerland) was inserted through the puncture, and 1 to 3 μl of 10^{12-13} vp/ml rAAV vectors in PBS was administered to the sub-retinal space, and a retinal detachment was induced. In particular, all co-injections were carried out at a plasmid molar ratio of 1:5 (AAV-IMPDH1 expressing plasmid: AAV-shRNA). Following sub-retinal injection, a reversing agent (100 μg/10 g body weight, Atipamezole Hydrochloride) was delivered by intraperitoneal injection. Body temperature was maintained using a homeothermic heating device.

Statistical analysis

For all experiments presented in this study: mean values, standard error of the mean (SEM) and paired Student's *t*-tests were calculated using Data Desk 6.0 PPC (Data Description, Inc., New York, NY, USA). Differences were considered statistically significant at *P*-values ≤ 0.05.

ACKNOWLEDGEMENTS

The authors would like to thank the following people for technical assistance: Dr Sara Bowne, University of Texas, Houston, for providing the IMPDH1 and IMPDH2 antibodies; Dr. Alfonso Blanco, Conway Institute, University College Dublin, Dublin, for assistance with FACS analysis and Sylvie Mehigan and Caroline Woods for animal husbandry.

Conflict of Interest statement. None declared.

FUNDING

The Ocular Genetics Unit at TCD is supported by grants from Science Foundation Ireland (G20026); The Health Research Board of Ireland (PRO262001); The Irish Research Council for Science, Engineering and Technology (IRCSET); European Union—RETNET (MRTN-CT-2003-504003); European Union—EviGenoRet (LSHG-CT-2005-512036); The British Retinitis Pigmentosa Society and Fighting Blindness Ireland.

REFERENCES

1. Hartong, D.T., Berson, E.L. and Dryja, T. (2006) Retinitis Pigmentosa. *Lancet*, **368**, 1795–1809.
2. Jordan, S.A., Farrar, G.J., Kenna, P.F., Humphries, M.M., Sheils, D.M., Kumar-Singh, R., Sharp, E.M., Ayuso, C., Benitez, J. and Humphries, P. (1993) Localization of an autosomal dominant retinitis pigmentosa gene to chromosome 7q. *Nat. Genet*., **4**, 54–58.
3. Kennan, A., Aherne, A., Palfi, A., Humphries, M., McKee, A., Stitt, A., Simpson, D.A., Demtroder, K., Orntoft, T., Ayuso, C. *et al.* (2002) Identification of an IMPDH1 mutation in autosomal dominant retinitis pigmentosa (RP10) revealed following comparative microarray analysis of transcripts derived from retinas of wild-type and Rho-/- mice. *Hum. Mol. Genet*., **11**, 547–557.
4. Bowne, S.J., Sullivan, L.S., Blanton, S.H., Cepko, C.L., Blackshaw, S., Birch, D.G., Hughbanks-Wheaton, D., Heckenlively, J.R. and Daiger, S.P. (2002) Mutations in the inosine monophosphate dehydrogenase 1 gene (IMPDH1) cause the RP10 form of autosomal dominant retinitis pigmentosa. *Hum. Mol. Genet*., **11**, 559–568
5. Natsumeda, Y., Ohno, S., Kawaski, H., Konno, Y., Weber, G. and And Susuki, K. (1990) Two distinct cDNAs for human IMP dehydrogenase. *J. Biol. Chem*., **265**, 5292–5295.
6. Carr, S.F., Papp, E., Wu, J.C. and And Natsumeda, Y. (1993) Characterisation of human type 1 and type II IMP dehydrogenase. *J Biol Chem*. **268**, 27286–27290.
7. Hager, P.W., Collart, F.R., Huberman, E. and Mitchell, B.S. (1995) Recombinant human inosine monophosphate dehydrogenase type I and type II proteins. Purification and characterization of inhibitor binding. *Biochem. Pharmacol*., **49**, 1323–1329.
8. Collart, F. and Huberman, E. (1988) Cloning and sequence analysis of the human and Chinese Hamster Inosine-5'-monophosphate dehygrogenase cDNAs. *J. Biol. Chem*., **263**, 15769–15772.
9. Nagai, M., Natsumeda, Y., Konno, Y., Hoffman, R., Irino, S. and Weber, G. (1991) Selective up-regulation of type II inosine 5'-monophosphate dehydrogenase messenger RNA expression in human leukemias. *Cancer Res*., **51**, 3886–3890.
10. Collart, F.R., Chubb, C.B., Mirkin, B.L. and Huberman, E. (1992) Increased inosine-5'-phosphate dehydrogenase gene expression in solid tumor tissues and tumor cell lines. *Cancer Res.*, **52**, 5826–5828.
11. Nagai, M., Natsumeda, Y. and Weber, G. (1992) Proliferation-linked regulation of type II IMP dehydrogenase gene in human normal lymphocytes and HL-60 leukemic cells. *Cancer Res*., **52**, 258–261.

12. Aherne, A., Kennan, A., Kenna, P.F., McNally, N., Lloyd, D.G., Alberts, I.L., Kiang, A.S., Humphries, M.M., Ayuso, C., Engel, P.C. *et al.* (2004) On the molecular pathology of neurodegeneration in IMPDH1-based retinitis pigmentosa. *Hum. Mol. Genet.*, **13**, 641–650.
13. McLean, J.E., Hamaguchi, N., Belenky, P., Mortimer, S.E., Stanton, M. and Hedstrom, L. (2004) Inosine 5́-monophosphate dehydrogenase binds nucleic acids *in vitro* and *in vivo*. *J. Biochem.*, **379**, 243–251.
14. Mortimer, S.E. and Hedstrom, L. (2005) Autosomal dominant retinitis pigmentosa mutations in inosine 5́-monophosphate dehydrogenase type I disrupt nucleic acid binding. *J. Biochem.*, **390**, 41–47.
15. Bowne, S.J., Liu, Q., Sullivan, L.S., Zhu, J., Spellicy, C.J., Rickman, C.B., Pierce, E.A. and Daiger, S.P. (2006) Why do mutations in the ubiquitously expressed housekeeping gene IMPDH1 cause retina-specific photoreceptor degeneration? *Invest. Ophthalmol. Vis. Sci.*, **47**, 3754–3765.
16. Sohocki, M.M., Daiger, S.P., Bowne, S.J., Rodriquez, J.A., Northrup, H., Heckenlively, J.R., Birch, D.G., Mintz-Hittner, H., Ruiz, R.S., Lewis, R.A. *et al.* (2001) Prevalence of mutations causing retinitis pigmentosa and other inherited retinopathies. *Hum Mutat.*, **17**, 42–51.
17. Reynolds, A., Leake, D., Boese, Q., Scaringe, S., Marshall, W.S. and Khovorova, A. (2004) Rational siRNA design for RNA interference. *Nat. Biotechnol.*, **22**, 326–330.
18. Elbashir, S.M., Harborth, J., Lendeckel, W., Yalcin, A., Weber, K. and Tuschl, T. (2001) Duplexes of 21-nucleotide RNAs mediate RNA interference in cultured mammalians cells. *Nature*, **411**: 494–498
19. Myers, J.W., Jr, Chi, J-T., Gong, D., Schaner, M.E., O'Brown, P. and Ferrell, J.E., Jr (2006) Minimizing off-target effects by diced siRNAs for RNA interference. *J. RNAi and Gene Silencing*, **2**. 181–194.
20. So, S., Nomura, Y., Adachi, N., Kobayashi, Y., Hori, T., Kurihara, Y. and Koyama, H. (2006) Enhanced gene targeting efficiency by siRNA that silences the expression of Bloom syndrome gene in human cells. *Gene to Cells*, **11**. 363–371.
21. Kiang, A.S., Palfi, A., Ader, M., Kenna, P.F., Millington-Ward, S., Clark, G., Kennan, A., O'Reilly, M., Tam, L.C.S., Aherne, A. *et al.* (2005) Toward a Gene Therapy for Dominant Disease: Validation of an RNA Interference-Based Mutation-Independent Approach. *Mol. Ther.*, **12**, 555–561.
22. Palfi, A., Arder, M., Kiang, A.S., Millington-Ward, S., Clark, G., O'Reilly, M., McMahon, H.P., Kenna, P.F., Humphries, P. and Farrar, G.J. (2006) RNAi-based suppression and replacement of rds-peripherin in retinal organotypic culture. *Hum. Mutat.*, **27**, 260–268.
23. O'Reilly, M., Palfi, A., Chadderton, N., Millington-Ward, S., Ader, M., Cronin, T., Tuohy, T., Auricchio, A., Hildinger, M., Tivnan, A. *et al.* (2007) RNA interference-mediated suppression and replacement of human rhodopsin *in vivo*. *Am. J. Hum. Genet.*, **81**, 127–135.
24. Xiao, X., Li, J. and Samulski, R.J. (1998) Production of high-titer recombinant adeno-associated virus vectors in the absence of helper adenovirus. *J. Virol.*, **72**, 2224–2232.
25. Hildinger, M., Auricchio, A., Gao, G., Wang, L., Chirmule, N. and Wilson, J.M. (2001) Hybrid vectors based on adeno-associated virus serotypes 2 and 5 for muscle-directed gene transfer. *J. Virol.*, **75**, 6199–6203.
26. Auricchio, A., Kobinger, G., Anand, V., Hildinger, M., O'Connor, E., Maguire, A.M., Wilson, J.M. and Bennett, J. (2001) Exchange of surface proteins impacts on viral vector cellular specificity and transduction characteristics: the retina as a model. *Hum. Mol. Genet.*, **10**, 3075–3081.
27. Tessitore, A., Parisi, F., Denti, M.A., Allocca, M., Di Vicino, U., Domenici, L., Bozzoni, I. and Auricchio, A. (2006) Preferential silencing of a common dominant rhodopsin mutation does not inhibit retinal degeneration in a transgenic model. *Mol. Ther.*, **14**, 692–699.
28. Gorbatyuk, M., Justilien, V., Liu, J., Hauswirth, W.W. and Lewin, A.S. (2007) Suppression of mouse rhodopsin expression in vivo by AAV mediated siRNA delivery. *Vis. Res.*, **47**, 1202–1208.
29. Humphries, M.M., Rancourt, D., Farrar, G.J., Kenna, P., Hazel, M., Bush, R.A., Sieving, P.A., Sheils, D.M., McNally, N., Creighton, P., Erven, A., Boros, A., Gulya, K., Capecchi, M.R. and Humphries, P. (1997) Retinopathy induced in mice by targeted disruption of the rhodopsin gene. *Nat. Genet.*, **15**: 216–219
30. Tan, E., Wang, Q., Quiambao, A.B., Xu, X., Qtaishat, N.M., Peachey, N.S., Lem, J., Fliesler, S.J., Pepperberg, D.R., Naash, M.I. and Al-Ubaidi, M.R. (2001) The relationship between opsin overexpression and photoreceptor degeneration, *Invest. Ophthal. Vis. Sci.*, **42**: 589–600
31. Cheng, T., Peachey, N.S., Li, S., Goto, Y., Cao, Y. and Naash, M.I. (1997) The effect of peripherin/rds haploinsufficiency on rod and cone photoreceptors. *J. Neurosci.*, **17**, 8118–8128
32. McNally, N., Kenna, P.F., Rancourt, D., Ahmed, T., Stitt, A., Colledge, W.H., Lloyd, D.G., Palfi, A., O'Neill, B., Humphries, M.M., Humphries, P. and Farrar, G.J. (2002) Murine model of autosomal dominant retinitis pigmentosa generated by targeted deletion at codon 307 of the rds-peripherin gene. *Hum. Mol. Genet.*, **11**: 1005–1016
33. Snyder, R.O., Miao, C., Meuse, L., Tubb, J., Donahue, B.A., Lin, H.F., Stafford, D.W., Patel, S., Thompson, A.R., Nichols, T. *et al.* (1999) Correction of hemophilia B in canine and murine models using recombinant adeno-associated viral vectors. *Nat. Med.*, **5**, 64–70.
34. Phillips, M.I., Tang, Y., Schmidt-Ott, K., Qian, K. and Kagiyama, S. (2002) Vigilant vector: heart-specific promoter in an adeno-associated virus vector for cardioprotection. *Hypertension*, **39**, 651–655.
35. Mount, J.D., Herzog, R.W., Tillson, D.M., Goodman, S.A., Robinson, N., McCleland, M.L., Bellinger, D., Nichols, T.C., Arruda, V.R., Lothrop, C.D., Jr. *et al.* (2002) Sustained phenotypic correction of hemophilia B dogs with a factor IX null mutation by liver-directed gene therapy. *Blood*, **99**, 2670–2676.
36. Ali, R.R., Sarra, G.M., Stephens, C., Alwis, M.D., Bainbridge, J.W., Munro, P.M., Fauser, S., Reichel, M.B., Kinnon, C., Hunt, D.M. *et al.* (2000) Restoration of photoreceptor ultrastructure and function in retinal degeneration slow mice by gene therapy. *Nat. Genet.*, **25**, 306–310.
37. Acland, G.M., Aguirre, G.D., Ray, J., Zhang, Q., Aleman, T.S., Cideciyan, A.V., Pearce-Kelling, S.E., Anand, V., Zeng, Y., Maguire, A.M. *et al.* (2001) Gene therapy restores vision in a canine model of childhood blindness. *Nat. Genet.*, **28**, 92–95.
38. Acland, G.M., Aguirre, G.D., Bennett, J., Aleman, T.S., Cideciyan, A.V., Bennicelli, J., Dejneka, N.S., Pearce-Kelling, S.E., Maguire, A.M., Palczewski, K. *et al.* (2005) Long-term restoration of rod and cone vision by single dose rAAV-mediated gene transfer to the retina in a canine model of childhood blindness. *Mol. Ther.*, **12**, 1072–1082.
39. Lotery, A.J., Yang, G.S., Mullins, R.F., Russell, S.R., Schmidt, M., Edwin, E.M., Lindbloom, J.D., Chiorini, J.A., Kotin, R.M. and Davidson, B.L. (2003) Adeno-associated virus type 5: Transduction efficiency and cell type specificity in the primate retina. *Hum. Gene Ther.*, **14**, 1663–1671.
40. Olsson, J.E., Gordon, J.W., Pawlyk, B.S., Roof, D., Hayes, A., Molday, R.S., Mukai, S., Cowley, G.S., Berson, E.L. and Dryja, T.P. (1992) Transgenic mice with rhodopsin mutation (Pro23His): A mouse model of autosomal dominant retinitis pigmentosa. *Neuron*, **9**, 815–830.
41. Cashman, S.M., Bowman, L., Christofferson, J. and Kumar-Singh, R. (2006) Inhibition of choroidal neovascularization by adenovirus-mediated delivery of short hairpin RNAs targeting VEGF as a potential therapy for AMD. *Invest. Ophthal. Vis. Sci.*, **47**, 3496–3504.
42. Illing, M.E., Rajan, R.S., Bence, N.F. and Kopito, R.R. (2002) A rhodopsin mutant linked to autosomal dominant retinitis pigmentosa is prone to aggregate and interacts with the ubiquitin proteasome system. *J. Biol. Chem.*, **277**, 34150–34160.
43. Rebello, G., Ramesar, R., Vorster, A., Roberts, L., Ehrenreich, L., Oppon, E., Gama, D., Bardien, S., Greenberg, J., Bonpapace *et al.* (2004) Apoptosis inducing signal sequence mutation in carbonic anhydrase IV indentified in patients with the RP17 form of retinitis pigmentosa. *Proc. Natl. Acad. Sci. USA*, **101**, 6617–6622.
44. Zoghbi, H.Y. and Orr, H.T. (2000) Glutamine repeats and neurodegeneration. *Annu. Rev. Neurosci.*, **23**, 217–247.
45. Nakamura, K., Jeong, S.Y., Uchihara, T., Anno, M., Nagashima, K., Nagashima, T., Ikeda, S., Tsuji, S. and Kanazawa, I. (2001) SCA17, a novel autosomal dominant cerebellar ataxia caused by an expanded polyglutamine in TATA-binding protein. *Hum. Mol. Genet.*, **10**, 1441–1448.
46. Xia, H., Mao, Q., Eliason, S.L., Harper, S.Q., Martins, I.H., Orr, H.T., Paulson, H.L., Yang, L., Kotin, R.M. and Davidson, B.L. (2004) RNAi suppresses polyglutamine-induced neurodegeneration in a model of spinocerebellar ataxia. *Nat. Med.*, **10**, 816–820.
47. Zimmermann, A.G., Spychala, J. and Mitchell, B.S. (1995) Characterization of the human inosine-5'-monophosphate dehydrogenase type II gene. *J. Biol. Chem.*, **270**, 6808–6814.
48. Gu, J.J., Spychala, J and Mitchell, B.S. (1997) Regulation of the Human Inosine Monophosphate Dehydrogenase Type I Gene. *J. Biol Chem.*, **272**, 4458–4466.

49. Semizarov, D., Kroeger, P. and Fesik, S. (2004) siRNA-mediated gene silencing: a global genome view. *Nucleic Acids Res*., **32**, 3838–3845.
50. Persengiev, S.P., Zhu, X. and Green, M.R. (2004) Nonspecific, concentration-dependent stimulation and repression of mammalian gene expression by small interfering RNAs (siRNAs). *RNA*, **10**, 12–18.
51. Sledz, C.A., Holko, M., de Veer, M.J, Silverman, R.H. and Williams, B.R. (2003) Activation of the interferon system by short interfering RNAs. *Nature Cell Biol*., **5**, 834–839.
52. Scacheri, P.C., Rozenblatt-Rosen, O., Caplen, N.J., Wolfsberg, T.G., Umayam, L., Lee, J.C., Hughes, C.M., Shanmugam, K.S., Bhattacharjee, A., Meryerson, M. *et al.* (2004) Short interfering RNAs can induce unexpected and divergent changes in the levels of untargeted proteins in mammalian cells. *Proc. Natl. Acad. Sci. USA*, **101**, 1892–1897.
53. Saxena, S., Jonsson, Z.O. and Dutta, A. (2003) Small RNAs with imperfect match to endogenous mRNA repress translation. Implications for off target activity of small inhibitory RNA in mammalian cells. *J. Biol. Chem*., **278**, 44312–44319.
54. Zeng, Y., Yi, R. and Cullen, B.R. (2003) MicroRNAs and small interfering RNAs can inhibit mRNA expression by similar mechanisms. *Proc. Natl. Acad. Sci. USA*, **100**, 9779–9784.
55. Jackson, A.L., Bartz, S.R., Schelter, J., Kobayashi, S.V., Burchard, J., Mao, M., Li, B., Cavet, G. and Linsley, P.S. (2003) Expression profiling reveals off target gene regulation by RNAi. *Nat. Biotechnol*., **21**, 635–637.
56. Reinhart, B.J., Slack, F.J., Basson, M., Pasquinelli, A.E., Bettinger, J.C., Rougvie, A.E., Horvitz, H.R. and Ruvkun, G. (2000) The 21-nucleotide let-7 RNA regulates developmental timing in Caenorhabditis elegans. *Nature*, **403**, 901–6.
57. Brennecke, J., Stark, A., Russell, R.B. and Cohen, S.M. (2005) Priniciples of microRNA-target recognition. *PLoS. Biol*., **3**, 404–418.
58. Kawasaki, H. and Taira, K. (2003) Hes1 is a target of microRNA-23 during retinoic-acid-induced neuronal differentiation of NT2 cells. *Nature*, **423**, 838–842.
59. Du, Q., Thonberg, H., Wang, J., Wahlestedt, C. and Liang, Z. (2005) A systematic analysis of the silencing effects of an active siRNA at all single-nucleotide mismatched target sites. *Nucleic Acids Res.*, **33**, 1671–1677.
60. Doench, J.G. and Sharp, P.A. (2004) Specificity of microRNA target selection translational repression. *Genes Dev.*, **18**, 504–511.
61. Lin, X., Ruan, X., Anderson, M.G., McDowell, J.A., Kroeger, P.E., Fesik, S.W. and Shen, Y. (2005) siRNA-mediated off target gene silencing triggered by a 7 nucleotide complementation. *Nucleic Acids Res*., **33**, 4527–4535.
62. Rolling, F. (2004) Recombinant AAV-mediated gene transfer to the retina: gene therapy perspectives. *Gene Ther*., **11**, 26–32.
63. Grimm, D., Streetz, K.L., Jopling, C.L., Storm, T.A., Pandey, K., Davies, C.R., Marion, P., Salazar, F. and Kay, M.A. (2006) Fatality in mice due to oversaturation of cellular microRNA/ short hairpin RNA pathways. *Nature*, **441**, 537–541.
64. Silva, J.M., Li, M.Z., Chang, K., Ge, W., Golding, M.C., Rickles, R.J., Siolas, D., Hu, G., Paddison, P.J., Schlabach, M.R. *et al.* (2006). Second-generation shRNA libraries covering the mouse and human genomes. *Nat. Genet.*, **37**, 1281–1284.
65. Castanotto, D., Sakurai, K., Lingeman, R., Li, H., Shively, L., Aagaard, L., Soifer, H., Gatignol, A., Riggs, A. and Rossi, J.J. (2007) Combinatorial delivery of small interfering RNAs reduces RNAi efficacy by selective incorporation into RISC. *Nuclei Acids Res.*, **35**, 5154–5164.
66. Brummelkamp, T.R., Bernards, R. and Agami, R. (2002) A system for stable expression of short interfering RNAs in mammalian cells. *Science*, **296**, 550–553
67. Rohr, U.P., Wulf, M.A., Stahn, S., Steidl, U., Haas, R. and Kronenwett, R. (2002) Fast and reliable titration of recombinant adeno-associated virus type-2 using quantitative real-time PCR. *J. Virol. Methods*, **106**, 81–88.